

Impedance of Beam Pipes with Smooth Shallow Corrugations

M. Dohlus
Deutsches Elektronen Synchrotron
Notkestr. 85, D-22603 Hamburg, Germany

Abstract

The beam impedance of monopole modes in a pipe with periodic, smooth and shallow corrugation has been calculated. The approach uses an orthogonal TM field expansion with Bessel functions and an impedance boundary condition, which takes into account resistive wall effects. The approach is valid for corrugations with period lengths larger, smaller and of the same order as the free space wavelength. The synergetic effect of the surface resistivity and sinusoidal or non-sinusoidal corrugations has been investigated. It is shown that these effects are nonlinear with respect to the beam impedance but they are well approximated by a superposition of the equivalent surface impedances. The concept of the equivalent surface impedance, which is directly related to the beam impedance, is introduced. Wake functions and wake potentials are calculated for several examples either by a pole expansion method (for perfect conducting surfaces) or by a Fourier transformation. The convergence of the approach is tested numerically and for one example the wake potential is compared with a direct numerical computation. The wake field effects due to surface roughness and conductivity in the TESLA-FEL beam pipe are estimated. This estimation takes into account statistical properties of a real measured surface.

1. Introduction

A new generation of accelerators, particularly linacs used as FEL drivers or for linear colliders, pushes the single bunch peak current into the kilo-Ampere regime. For example, in the TESLA SASE FEL the peak current is 5kA, the rms bunch length is 25 μm and the normalized emittance is 1.6 mrad mm. The gain length is of the order of 10...20 m and the undulator has a length of about 15 times the gain length. In small beam pipes with a radius of a few mm induced wakefields may significantly increase the beam energy spread or the emittance, and may interfere with the FEL process. A larger beam pipe radius reduces the wakefields but it also reduces the achievable undulator field strength so that the gain length, the undulator length and the costs are increased. The sources of wakefields are the discontinuities of the beam pipe (e.g. for diagnostics and the vacuum system) and the surface resistivity and roughness. Based on the model of a periodically corrugated beam pipe we estimate the monopole wakes caused by the resistivity and the surface roughness.

At present different models have been developed by K.Bane, C.Ng, A.Chao [1], G.Stupakov [2], A.Novokhatski, M.Timm, T.Weiland [3] to study the effect of a random surface roughness in a beam pipe, and by K.Bane, A.Novokhatski [4], G.Stupakov [5] to calculate the wake in beam pipes with periodic surface structure. These models are based on the assumption that all dimensions of the surface structure (typical wavelength and amplitude) are small compared to the bunch length. This is not necessarily fulfilled by real surfaces (e.g. [6]). Based on a simple TM field

expansion with Bessel functions we calculate the beam impedance for smooth and shallow corrugations of any period length. Usually such approaches are made for systems of cylindrical pipes with piecewise constant radius. Therefore the calculation domain is split into several segments with a field expansion for each segment. The matching conditions at the interface planes lead to an infinite equation system, which is usually truncated and solved numerically. For smooth and shallow corrugations this approach can be significantly simplified because the boundary conditions at the pipe surface can be fulfilled by only one field expansion for the whole domain. Even an impedance boundary condition, which takes into account resistive wall losses, can be considered without additional effort.

There are several methods to approximate the boundary condition by a truncated Rayleigh expansion with $2N + 1$ basis fields. The $2N + 1$ unknown coefficients can be calculated so that the rms error at the boundary is minimal (RMS- N approximation) or that the lowest $2N + 1$ Fourier coefficients of the boundary error vanish (Fourier- N approximation) or so that the Fourier coefficients of a linear boundary approximation vanish (LB- N approximation). The beam impedance is linearly related to one of these coefficients. Another useful quantity is the equivalent surface impedance. It is defined by the quotient of the Fourier amplitudes of the longitudinal electric field $\int E_z(R, z) \exp(jk_0 z) dz$ and the azimuthal magnetic field $\int H_\varphi(R, z) \exp(jk_0 z) dz$ at the minimal pipe radius. There exists a simple transformation that relates the beam and the surface impedance and there is also a matrix transformation (for the coefficients of the Rayleigh expansion) so that the surface impedance is linearly related to one of the transformed coefficients. The transformed equation system is more suitable for a 1st order matrix inversion by which an explicit formulation for the impedance is derived (LB- $N, 2^{\text{nd}}$ approximation).

For several examples the beam impedance, the wake function or the wake potential is calculated for sinusoidal corrugations. The beam impedance calculated by the LB-1 approximation agrees well with the results of higher order approximations for frequencies below c_0/λ (with λ the corrugation wavelength). There is also an agreement at higher frequencies with the exception of numerous very weak additional resonances which are missed by the LB-1 approximation. These resonances have almost no effect to the short range wake. Therefore the wake potentials calculated by the LB-1 method and the RMS-5 method agree well. A good agreement is also found for a non-sinusoidal surface. In contrast to this, the direct superposition of the resistive wall wake (without corrugation) and of the wakes of sinusoidal corrugations (for perfect electric boundary conditions) gives a significantly different result.

The measured surface structure of a $720 \times 720 \mu\text{m}$ sample is used to estimate the wakefield effects in an undulator beam pipe. This is possible with a formulation of the LB- $N, 2^{\text{nd}}$ approximation that depends not explicitly on a surface periodicity but on the spectral power density of the surface function. Therefore the 2D- and 1D-autocorrelation functions are computed and extrapolated to determine the spectral power density by a Fourier transformation. The wakes of gaussian bunches with rms length $25 \mu\text{m}$ in copper plated beam pipes with radii between 3 and 6 mm are approximately 23% larger than in a resistive pipe without surface roughness. A similar result is found for bunches with a more rectangular shape.

2. Analytical Approach

We consider an infinite axially symmetric beam pipe with the z -dependent radius $R(z) = R_0 + \delta r(z)$. R_0 is the averaged radius, the surface function $\delta r(z) = \delta r(z + \lambda)$ describes a periodic perturbation of the pipe radius with the period length λ . The surface function has to be smooth (so that the EM fields are non singular) and it has to be shallow (so that the field expansion, described in the following, converges). For $0 < r < R(z)$ the EM fields have to fulfil the wave equation

$$\left(\nabla^2 + k_0^2\right)\left(E_r \vec{e}_r + E_z \vec{e}_z\right) = \vec{0}, \quad \left(\nabla^2 + k_0^2\right)\left(H_\varphi \vec{e}_\varphi\right) = \vec{0} \quad (1)$$

and the conditions $\text{div } \vec{E} = 0$, $\text{div } \vec{H} = 0$. An impedance boundary condition is used at the surface of the corrugation: $-\vec{E} \times \vec{n} = Z_b \vec{H}$. The boundary impedance Z_b relates the longitudinal electric field and the azimuthal magnetic field. In general Z_b depends on the EM fields which are unknown. Only for beam pipes without corrugation can it be shown that Z_b is quite well approximated by its asymptotical value for $R_0 \rightarrow \infty$:

$$Z_b(\omega) = \sqrt{(j\omega\mu)/(\sigma + j\omega\epsilon)}, \quad (2)$$

with σ the electric conductivity. In the following we use this approximation even for corrugated pipes. The frequency dependent conductivity is $\sigma(\omega) = \sigma_0/(1 + j\omega\tau)$ with $\sigma_0 = 36.6 \cdot 10^6/\Omega\text{m}$, $\tau = 0.71 \cdot 10^{-14}$ s for aluminum and $\sigma_0 = 57 \cdot 10^6/\Omega\text{m}$, $\tau = 2.46 \cdot 10^{-14}$ s for copper. This boundary condition is equivalent to:

$$\nabla H_\varphi \cdot \vec{n} = -(j\omega\epsilon_0 Z_b + (\vec{e}_r \cdot \vec{n})/R) H_\varphi, \quad (3)$$

with $\varphi(z) = \arctan(\partial_z \delta r(z))$ and $\vec{n} = -\sin(\varphi(z))\vec{e}_z + \cos(\varphi(z))\vec{e}_r$. The source of the EM fields is an ultrarelativistic beam on the z -axis (approximations: $v \rightarrow c_0$, no transverse dimensions):

$$\begin{aligned} \rho(\vec{r}, \omega) &= \delta(\vec{r} \cdot \vec{e}_x) \delta(\vec{r} \cdot \vec{e}_y) \exp(-jk_0 z) I(\omega)/c_0 \\ \vec{J}(\vec{r}, \omega) &= \delta(\vec{r} \cdot \vec{e}_x) \delta(\vec{r} \cdot \vec{e}_y) \exp(-jk_0 z) \vec{e}_z I(\omega) \end{aligned} \quad (4)$$

with the wavenumber $k_0 = \omega/c_0$ and the beam current $I(\omega)$ in the frequency domain. The electromagnetic fields are approximated by a truncated field expansion with $2N + 1$ basis fields:

$$\begin{aligned} H_\varphi &= H_{\varphi a} + \sum_n C_n H_{\varphi n} \\ E_r &= E_{ra} + \sum_n C_n E_{rn} \quad , \\ E_z &= E_{za} + \sum_n C_n E_{zn} \end{aligned} \quad (5)$$

with

$$H_{\varphi a} = \frac{I}{2\pi r} \exp(-jk_{z,0}z)$$

$$H_{\varphi n} = \begin{cases} \frac{r}{2} \exp(-jk_{z,0}z) & \text{if } n=0 \\ \frac{J'_0(k_{r,n}r)}{k_{r,n}} \exp(-jk_{z,n}z) & \text{otherwise} \end{cases}, \quad (6)$$

$$E_{ra} = \frac{IZ_0}{2\pi r} \exp(-jk_{z,0}z)$$

$$E_m = \begin{cases} Z_0 \frac{r}{2} \exp(-jk_{z,0}z) & \text{if } n=0 \\ \frac{k_{zn}}{\omega\epsilon_0} \frac{J'_0(k_{r,n}r)}{k_{r,n}} \exp(-jk_{z,n}z) & \text{otherwise} \end{cases}, \quad (7)$$

$$E_{za} = 0$$

$$E_{zn} = \begin{cases} -\frac{1}{j\omega\epsilon_0} \exp(-jk_{z,0}z) & \text{if } n=0 \\ -\frac{1}{j\omega\epsilon_0} J_0(k_{r,n}r) \exp(-jk_{z,n}z) & \text{otherwise} \end{cases} \quad (8)$$

and $n = -N, \dots, N$, $k_1 = 2\pi/\lambda$, $k_{z,n} = k_0 + nk_1$, $k_{r,n} = \sqrt{k_0^2 - k_{z,n}^2}$. The basis field $\{E_{ra}, E_{za}, H_{\varphi a}\}$ fulfils Maxwell's equations and the boundary condition at $r=0$, the other basis fields $\{E_m, E_{zn}, H_{\varphi n}\}$ also fulfil Maxwell's equations and the homogeneous boundary condition at the origin. This field expansion converges for all $r \leq \min(R(z))$, but for smooth and shallow boundary perturbations it is even possible to fulfil the outer boundary condition. Therefore the expansion coefficients C_n have to be chosen so that the error at the outer boundary is minimized:

$$d(z) := h_a(z) + \sum_n C_n h_n(z) \rightarrow 0, \quad (9)$$

with

$$h_a(z) = \left\{ \nabla H_{\varphi,a} \cdot \vec{n} + (j\omega\epsilon_0 Z_b + (\vec{e}_r \cdot \vec{n})/R) H_{\varphi,a} \right\}_{R=R(z)}$$

$$h_n(z) = \left\{ \nabla H_{\varphi,n} \cdot \vec{n} + (j\omega\epsilon_0 Z_b + (\vec{e}_r \cdot \vec{n})/R) H_{\varphi,n} \right\}_{R=R(z)} \quad (10)$$

or

$$h_a(z) = \frac{I}{2\pi R(z)} (jk_{z,0} \sin(\varphi(z)) + j\omega\epsilon_0 Z_b) \exp(-jk_{z,0}z)$$

$$h_0(z) = \left(\cos(\varphi(z)) + \frac{R(z)}{2} (jk_{z,0} \sin(\varphi(z)) + j\omega\epsilon_0 Z_b) \right) \exp(-jk_{z,0}z) \quad (11)$$

$$h_{n \neq 0}(z) = - \left(J_0(k_{r,n}R(z)) \cos(\varphi(z)) + \frac{J_1(k_{r,n}R(z))}{k_{r,n}} (jk_{z,n} \sin(\varphi(z)) + j\omega\epsilon_0 Z_b) \right) \exp(-jk_{z,n}z)$$

The beam impedance (per length) relates the z -averaged longitudinal electric field to the beam current:

$$Z_{\text{beam}}(\omega) = -\frac{\langle E_z(r, z)e^{jk_0z} \rangle_z}{I} = \frac{1}{j\omega\epsilon_0} \frac{C_0}{I}. \quad (12)$$

As we are considering only monopole modes, this quantity is independent of the radial offset r of the integration. In this report the sign of the beam impedance is defined so that the wake function

$$W(s) = \frac{1}{2\pi} \int Z_{\text{beam}}(\omega) \exp(js\omega/c_0) d\omega \quad (13)$$

is negative for infinitely small values of s . Therefore the **negative** beam impedance has the properties of a two-terminal network [7].

2.1. Solution of the Boundary Problem

One possibility to approximate Eq. (9) is to minimize the RMS error at certain boundary points $(R(z_i), z_i)$ with $1 \leq i \leq I$ and $0 \leq z_i < \lambda$:

$$\sum_i |d_i - d(z_i)|^2 \rightarrow \min. \quad (14)$$

This is equivalent to the matrix equation

$$\|\mathbf{M}\mathbf{c} + \mathbf{v}\| \rightarrow \min \quad (15)$$

with

$$(\mathbf{M})_{i,\hat{n}} = h_n(z_i), (\mathbf{c})_{\hat{n}} = C_n \text{ and } (\mathbf{v})_i = h_a(z_i). \quad (16)$$

The indices n and later m are shifted to $\hat{n} = n + N + 1$, $\hat{m} = m + N + 1$ so that the numbering of matrix rows and columns starts at 1. The mathematics to solve Eq. (15) is well known so that it is not described here. In the following we denote the beam impedance calculated by Eqs. (12, 15) as **RMS- N approximation**. Another method is to fulfil Eq. (9) for the Fourier coefficients $\tilde{d}_m = F_m\{d(z)\}$ with $m = -N, \dots, N$ and

$$F_m\{d(z)\} = \frac{1}{\lambda} \int_0^\lambda d(z) \exp(jmk_1z) dz. \quad (17)$$

This leads to the linear equation

$$\tilde{\mathbf{M}}\mathbf{c} + \tilde{\mathbf{v}} = \mathbf{0} \quad (18)$$

with

$$(\tilde{\mathbf{M}})_{\hat{m},\hat{n}} = F_m\{h_n(z)\} \text{ and } (\tilde{\mathbf{v}})_{\hat{m}} = F_m\{h_a(z)\}. \quad (19)$$

In the general case the Fourier integration cannot be done analytically but it has to be solved on a discrete mesh $0 \leq z_i < \lambda$. The beam impedance calculated by Eqs. (12,18) is denoted in this report as **Fourier- N approximation**.

For loss-free boundaries ($Z_b = 0$) and even surface functions ($\delta r(z) = \delta r(-z)$) it can be shown that the real parts of h_a and h_n are even and the imaginary parts odd

functions. Therefore the coefficients C_n are real numbers and the beam impedance Eq. (12) is purely imaginary.

2.2. Equivalent Surface Impedance

Originally the boundary impedance $Z_b(j\omega)$ is defined as the ratio of the longitudinal electrical field to the azimuthal magnetic field on the surface of a pipe with constant radius R_0 . For corrugated beam pipes we define a similar quantity, **the equivalent surface impedance**, as the quotient of the Fourier amplitudes of the longitudinal electrical field and the azimuthal magnetic field at the minimal pipe radius:

$$Z_s(\omega) = \frac{\left\langle E_z(\min(R), z) e^{jk_0 z} \right\rangle_z}{\left\langle H_\varphi(\min(R), z) e^{jk_0 z} \right\rangle_z}. \quad (20)$$

By substitution of Eq. (6) and (8) it follows immediately that

$$Z_s(\omega) = \frac{-\frac{1}{j\omega\epsilon_0} C_0}{\frac{I}{2\pi \min(R)} + \frac{\min(R)}{2} C_0}. \quad (21)$$

For simplicity we use in the following: $\min(R) = R_0 + \min(\delta r) \approx R_0$. The equivalent surface impedance and the beam impedance Eq. (12) are related by

$$Z_s(\omega) = -2\pi R_0 \frac{Z_{\text{beam}}(\omega)}{1 + j\omega\epsilon_0 \pi R_0^2 Z_{\text{beam}}(\omega)}, \quad (22a)$$

$$Z_{\text{beam}}(\omega) = -\frac{1}{2\pi R_0} \frac{Z_s(\omega)}{1 + j\omega\epsilon_0 \frac{R_0}{2} Z_s(\omega)}. \quad (22b)$$

The equivalent surface impedance can be calculated directly from a transformation of the matrix equation (19) as

$$Z_s(\omega) = -\frac{1}{j\omega\epsilon_0} \frac{\hat{C}_0}{I}, \quad (23a)$$

with

$$\begin{aligned} \hat{C}_n &= (\hat{\mathbf{c}})_{\hat{n}} \\ \hat{\mathbf{c}} &= -2\pi R_0 \hat{\mathbf{M}}^{-1} \tilde{\mathbf{v}} \\ (\hat{\mathbf{M}})_{\hat{m}, \hat{n}} &= \begin{cases} (\tilde{\mathbf{M}})_{\hat{m}, \hat{n}} - (\tilde{\mathbf{v}})_{\hat{m}} \pi R_0^2 / I & \text{if } n = 0 \\ (\tilde{\mathbf{M}})_{\hat{m}, \hat{n}} & \text{otherwise} \end{cases} \end{aligned} \quad (23b)$$

It is interesting to notice that the negative beam impedance can be written as a parallel connection of the capacitance $C = \epsilon_0 \pi R_0^2$ and the impedance $Z_s(\omega)/2\pi R_0$ (cf. Fig. 1a). The energy loss per length of a point particle with the charge q is

$$-W(0+)q^2 = k_{\text{tot}} q^2 = \frac{1}{2} \frac{q^2}{C_k} \quad (24)$$

with k_{tot} the total loss-parameter and C_k the maximal parallel capacitance which can be extracted from $-Z_{\text{beam}}$, so that the residual impedance still has the properties of a two-terminal network. Supposing no parallel capacitance can be extracted from Z_s , the total loss-parameter is

$$k_{tot} = \frac{1}{2C} = \frac{1}{\epsilon_0 2\pi R_0^2}. \quad (25)$$

For example this is the case if Z_s can be expressed as a series connection of a two-terminal network with an inductance $j\omega L$ or as an infinite sum of parallel LC circuits $\sum j\omega\alpha_n/(\omega_{s,n}^2 - \omega^2)$ where the sum of pole coefficients is divergent (cf. Fig. 1b):

$$\sum \alpha_n \rightarrow \infty. \quad (26)$$

2.3. Linear Boundary Approximation

The boundary functions $h_a(z)$ and $h_n(z)$ can be linearized with respect to δr by a substitution of the following approximation

$$\begin{aligned} \cos(\varphi(z)) &\approx 1 \\ J_0(k_{r,n}R(z)) &\approx J_0(k_{r,n}R_0) - J_1(k_{r,n}R_0)k_{r,n}\delta r(z) \\ J_1(k_{r,n}R(z))\sin(\varphi(z)) &\approx J_1(k_{r,n}R_0)\delta r'(z) \\ J_1(k_{r,n}R(z))Z_b &\approx (J_1(k_{r,n}R_0)(1 - \delta r(z)/R_0) + k_{r,n}\delta r(z)J_0(k_{r,n}R_0))Z_b \\ R_0/R &\approx 1 - \delta r/R_0 \end{aligned} \quad (27)$$

into Eq. (11):

$$\begin{aligned} h_a(z) &= \frac{I}{2\pi R_0} (jk_{z,0}\delta r' + (1 - \delta r/R_0)j\omega\epsilon_0 Z_b) \exp(-jk_{z,0}z) \\ h_0(z) &= \left(1 + jk_{z,0} \frac{R_0}{2} \delta r' + \frac{R_0 + \delta r}{2} j\omega\epsilon_0 Z_b \right) \exp(-jk_{z,0}z) \\ h_{n \neq 0}(z) &= - \left(J_0(k_{r,n}R_0)(1 + \delta r j\omega\epsilon_0 Z_b) + J_1(k_{r,n}R_0) \times \right. \\ &\quad \left. \times \left(j \frac{k_{z,n}}{k_{r,n}} \delta r' - k_{r,n} \delta r + \frac{(1 - \delta r/R_0)}{k_{r,n}} j\omega\epsilon_0 Z_b \right) \right) \exp(-jk_{z,n}z) \end{aligned} \quad (28)$$

This approximation is valid if $\delta r \ll R_0$, $\delta r' \approx \varphi \ll 1$ and $|k_{r,n}\delta r| \ll 1$. The last condition is fulfilled if $2\pi \max(|n\delta r|) \ll \lambda$. Therefore this approximation can be used for field expansions that converge with $N \ll \lambda/\max(2\pi|\delta r|)$. To avoid the $\exp(-jk_{z,0}z)$ term in $h_a(z)$ and $h_0(z)$ we multiply the inverse factor (which is $\exp(jk_0z)$) with the boundary Eq. (9) and get

$$\begin{aligned}
\hat{d}(z) &:= \hat{h}_a(z) + \sum_n C_n \hat{h}_n(z) \rightarrow 0 \\
\hat{d}(z) &= d(z) \exp(jk_0 z) \\
\hat{h}_a(z) &= h_a(z) \exp(jk_0 z) \\
\hat{h}_n(z) &= h_n(z) \exp(jk_0 z)
\end{aligned} \tag{29}$$

For these modified boundary functions the Fourier coefficients, which are identical to the matrix elements in Eq. (19), are explicitly given as:

$$\begin{aligned}
F_m \{\hat{h}_a(z)\} &= \delta_{0,m} \frac{I}{2\pi R_0} j\omega \epsilon_0 Z_b + F_m \{\delta r\} \frac{I}{2\pi R_0} \left(mk_1 k_0 - \frac{1}{R_0} j\omega \epsilon_0 Z_b \right) \\
F_m \{\hat{h}_0(z)\} &= \delta_{0,m} \left(1 + j\omega \epsilon_0 Z_b \frac{R_0}{2} \right) + F_m \{\delta r\} \frac{1}{2} (R_0 m k_1 k_0 + j\omega \epsilon_0 Z_b) \quad , \quad (30) \\
F_m \{\hat{h}_{n \neq 0}(z)\} &= -\delta_{n,m} \left(J_0(k_{r,n} R_0) + \frac{j\omega \epsilon_0 Z_b}{k_m} J_1(k_{r,n} R_0) \right) \\
&\quad - F_{m-n} \{\delta r\} \left(J_0(k_{r,n} R_0) j\omega \epsilon_0 Z_b + \frac{J_1(k_{r,n} R_0)}{k_{r,n}} \times \right. \\
&\quad \left. \times \left((m+n)k_0 k_1 + nmk_1^2 - \frac{j\omega \epsilon_0 Z_b}{R_0} \right) \right)
\end{aligned}$$

with $\delta_{n,m}$ the Kronecker delta function. The beam impedance calculated with the linear boundary approximation and by Eqs. (12,18) is denoted as **LB-N approximation**.

2.4. Pipe with Sinusoidal Corrugation and Perfect Electric Conductivity (PEC)

The Fourier coefficients of the surface function $\delta r = a \cos(zk_1)$ of a pipe with sinusoidal corrugation are:

$$F_m \{\delta r\} = \begin{cases} a/2 & \text{if } |m|=1 \\ 0 & \text{otherwise} \end{cases} \tag{31}$$

Therefore the matrix equation (18) has the following form for $N=1$ and a beam pipe with perfect electric conductivity ($Z_b = 0$):

$$\begin{bmatrix} -J_0(k_{r,-1} R_0) & -\frac{k_1 k_0 R_0}{2} \frac{a}{2} & 0 \\ J_1(k_{r,-1} R_0) \frac{a}{2} \frac{k_1 k_0}{k_{r,-1}} & 1 & -J_1(k_{r,1} R_0) \frac{a}{2} \frac{k_1 k_0}{k_{r,1}} \\ 0 & \frac{k_1 k_0 R_0}{2} \frac{a}{2} & -J_0(k_{r,1} R_0) \end{bmatrix} \begin{bmatrix} C_{-1} \\ C_0 \\ C_1 \end{bmatrix} + \begin{bmatrix} -\frac{Ik_1 k_0}{2\pi R} \frac{a}{2} \\ 0 \\ \frac{Ik_1 k_0}{2\pi R} \frac{a}{2} \end{bmatrix} = \mathbf{0} \tag{32}$$

The equivalent surface impedance follows with Eq. (23) as

$$Z_{s,PEC}(\omega) = jk_0 Z_0 \frac{(ak_1)^2}{4} \left(\frac{J_1(k_{r,-1} R)}{J_0(k_{r,-1} R) k_{r,-1}} + \frac{J_1(k_{r,1} R)}{J_0(k_{r,1} R) k_{r,1}} \right) \tag{33}$$

Eq. (22b) with Eq. (33) is the **LB-1 approximation** of the beam impedance for PEC corrugations.

The total loss-parameter: Using the relation

$$\frac{J_1(x)}{J_0(x)x} = \sum_{n=1}^{\infty} \frac{2}{j_{0,n}^2 - x^2}, \quad (34)$$

with $j_{0,n}$ the roots of $J_0(x)$, Eq. (33) can be expressed as a pole expansion

$$Z_{s,\text{PEC}}(\omega) = \sum_{n=1}^{\infty} j\omega\alpha_n / (\omega_{s,n}^2 - \omega^2), \quad (35)$$

with the pole frequencies and pole coefficients

$$\begin{aligned} \omega_{s,n} &= \frac{k_1 c_0}{2} + j_{0,n}^2 \frac{c_0}{2R_0^2 k_1} \\ \alpha_n &= \frac{1}{\varepsilon_0 R_0} \left(\frac{ak_1}{2} \right)^2 \left(1 + \left(\frac{j_{0,n}}{Rk_1} \right)^2 \right) \end{aligned} \quad (36)$$

It is easy to see that the criterion Eq. (26) is fulfilled which means the total loss-parameter k_{tot} is $1/\varepsilon_0 2\pi R_0^2$.

Wake function and wake potential: As the equivalent surface impedance can be described by a LC network the negative beam impedance has the same property (cf. Fig. 1b,c). Therefore the beam impedance can be written in the following form:

$$Z_{\text{beam,PEC}}(\omega) = -2 \sum_{n=1}^{\infty} j\omega k_n / (\omega_n^2 - \omega^2), \quad (37)$$

with the loss-parameters k_n and the pole frequencies ω_n . The pole parameters k_n , ω_n have to be calculated numerically from Eqs. (22b, 35). The wake function is

$$W(s) = - \sum_{n=1}^{\infty} k_n \cos(s\omega_n/c_0) \begin{cases} 0 & \text{for } s < 0 \\ 1 & \text{for } s = 0 \\ 2 & \text{otherwise} \end{cases} \quad (38)$$

and the wake potential for a Gaussian bunch with the rms length σ is given by the convolution

$$W^\sigma(s) = \int W(s-x) \frac{g(x/\sigma)}{\sigma} dx \quad (39)$$

with $g(x)$ the Gaussian normal distribution. In a numerical analysis it is not possible to calculate the infinite series of pole parameters and to perform the infinite summation, but one can take into account so many resonances that the truncated sum of loss-parameters approaches

$$\sum_{n=1}^{\infty} k_n = k_{tot} = 1/\varepsilon_0 2\pi R_0^2. \quad (40)$$

Another possibility is to calculate only the pole parameters in the spectrum of the beam $I(\omega)$ and to split the beam impedance into two parts

$$Z_1(\omega) = -2 \sum_{n=1}^{N_{\max}} j\omega k_n / (\omega_n^2 - \omega^2),$$

$$Z_2(\omega) = Z_{\text{beam,PEC}}(\omega) - Z_1(\omega),$$

which can be evaluated numerically ($Z_{\text{beam,PEC}}$ is given by Eqs. (22b, 33)). The contribution of the first part to the wake potential can be computed as before (inverse Fourier transformation of Z_1 , convolution). $Z_2(\omega)$ is smooth and non-singular for all frequencies in the beam spectrum. Therefore the contribution of the second part can be calculated by the inverse Fourier transformation of $Z_2(\omega)I(\omega)$. In many cases the second contribution is negligible.

It is interesting to compare Eq. (33) with the equivalent surface impedance of a planar corrugation

$$Z_{\text{s,PEC,plane}}(j\omega) = jk_0 Z_0 \frac{(ak_1)^2}{4} \left(\frac{j}{k_{r,-1}} + \frac{j}{k_{r,1}} \right). \quad (41)$$

This formula is derived in [5] with similar approximations as used for Eq. (33). Both formulas are in excellent agreement for $\omega < \pi c_0 / \lambda =: \omega_\lambda$. For one example the beam impedances calculated by the LB-1 approximation and by Eqs. (22b,41) are compared in Fig. 2. The first pole of the beam impedance is well approximated, but it can be seen in Fig. 3 that there are many further poles above ω_λ . Approximation Eq. (41) can be used for the calculation of the wake function $W^\sigma(s)$ if the bunch spectrum is negligible for frequencies above ω_λ . The pole sum $K_n = \sum_{m=1}^n k_m$ is plotted in Fig. 4 as function of the pole frequencies. For the given geometry parameters the higher poles ($n > 1$) contribute significantly to the impedance and the wake function in Fig. 5.

2.5. Pipe with Sinusoidal Corrugation and Finite Conductivity

For finite surface conductivity the matrix equation (18) has the following form

$$(\mathbf{M}_0 + a\mathbf{M}_a + j\omega\epsilon_0 Z_b \mathbf{M}_Z) \begin{bmatrix} C_{-1} \\ C_0 \\ C_1 \end{bmatrix} + \frac{I}{2\pi R_0} \begin{bmatrix} \frac{a}{2}(-k_1 k_0 - j\omega\epsilon_0 Z_b / R_0) \\ j\omega\epsilon_0 Z_b \\ \frac{a}{2}(k_1 k_0 - j\omega\epsilon_0 Z_b / R_0) \end{bmatrix} = \mathbf{0}$$

$$\mathbf{M}_0 = \begin{bmatrix} -J_0(k_{r,-1} R_0) & 0 & 0 \\ 0 & 1 & 0 \\ 0 & 0 & -J_0(k_{r,1} R_0) \end{bmatrix} \quad (42a)$$

$$\mathbf{M}_a = \frac{k_1 k_0}{4} \begin{bmatrix} 0 & -R_0 & 0 \\ 2 \frac{J_1(k_{r,-1} R_0)}{k_{r,-1}} & 0 & -2 \frac{J_1(k_{r,1} R_0)}{k_{r,1}} \\ 0 & R_0 & 0 \end{bmatrix}$$

$$\mathbf{M}_Z = \begin{bmatrix} -\frac{J_1(k_{r,-1}R_0)}{k_{r,-1}R_0} & \frac{a}{4} & 0 \\ -\frac{a}{2} \left(J_0(k_{r,-1}R_0) - \frac{J_1(k_{r,-1}R_0)}{k_{r,-1}} \right) & \frac{R_0}{2} & -\frac{a}{2} \left(J_0(k_{r,1}R_0) - \frac{J_1(k_{r,1}R_0)}{k_{r,1}} \right) \\ 0 & \frac{a}{4} & -\frac{J_1(k_{r,1}R_0)}{k_{r,1}R_0} \end{bmatrix} \quad (42b)$$

Eq. (12) with C_0 calculated by Eq. (42) is the general formulation of the **LB-1 approximation**. The equivalent surface impedance can be written as the sum of the boundary impedance, the equivalent surface impedance for PEC boundary conditions and a residual term of the order $a^2 Z_b$:

$$Z_s(\omega) = Z_b(\omega) + Z_{s,\text{PEC}}(\omega) + O(a^2 Z_b).$$

For an aluminum beam pipe with radius $R_0 = 5\text{ mm}$ and sinusoidal corrugation $\delta r(z) = a \cos(2\pi z/\lambda)$, $a = 1\ \mu\text{m}$, $\lambda = 50\ \mu\text{m}$ the normalized boundary error, defined as

$$\|\mathbf{M}\mathbf{c} + \mathbf{v}\|/\|\mathbf{v}\|,$$

is calculated by the RMS-5 approximation. In Fig. 6 this error can be seen in the frequency range $0 \dots f_\lambda$. For frequencies close to the first resonance ($\approx 0.86 f_\lambda$) the error is of the order of 10^{-7} , for the rest of the frequency range it is well below this value. This is similar in Fig. 7 with the error in a narrow frequency range around one of the next resonances. In Fig. 8 and 9 the beam impedance is calculated for the same frequency ranges by the RMS-5 and LB-1 method. Both methods are found to be in excellent agreement.

The impedance and wake function of a corrugated pipe with PEC boundary and finite conducting boundary are compared in Figs. 10, 11 and 12. The wake potential of a gaussian bunch with $\sigma_s = 25\ \mu\text{m}$ is shown in Fig. 13 for the same example. (In this report all wake potentials of pipes with finite conductivity are calculated by the inverse Fourier transformation of $Z_{\text{beam}}(\omega)I(\omega)$.) For this setup the wake potential of a corrugated surface with finite conductivity is only roughly described by the sum of the wake potential of a surface with PEC boundary condition and the resistive wall wake potential of a pipe without corrugation. This can also be seen in Fig. 14 with the wake potentials of a surface with different corrugation.

2.6. Non-sinusoidal Corrugations

The beam impedance of periodic, non-sinusoidal corrugations can be calculated with the RMS- N , Fourier- N or LB- N approximation. In the following an explicit 2nd order approximation of the impedance is derived. Therefore the matrix $\hat{\mathbf{M}}$ in Eq. (23) is split into a diagonal matrix $\hat{\mathbf{D}}$ with main diagonal of $\hat{\mathbf{M}}$ and a residual matrix $\hat{\mathbf{W}}$:

$$\hat{\mathbf{M}} = \hat{\mathbf{D}} + \hat{\mathbf{W}}, \quad (43)$$

$$\begin{aligned}
(\hat{\mathbf{D}})_{\hat{n},\hat{n}} &= \begin{cases} 1 & \text{if } n = 0 \\ -J_0(k_{r,n}R_0) - \frac{j\omega\epsilon_0 Z_b}{k_m} J_1(k_{r,n}R_0) & \text{otherwise} \end{cases} \\
(\hat{\mathbf{W}})_{\hat{m},\hat{n}} &= \begin{cases} F_m \{\delta r\} j\omega\epsilon_0 Z_b & \text{if } n = 0 \\ -F_{m-n} \{\delta r\} X_{m,n} & \text{otherwise} \end{cases} \\
X_{m,n} &= J_0(k_{r,n}R_0) j\omega\epsilon_0 Z_b + \frac{J_1(k_{r,n}R_0)}{k_{r,n}} \left((m+n)k_0 k_1 + nm k_1^2 - \frac{j\omega\epsilon_0 Z_b}{R_0} \right)
\end{aligned} \quad . \quad (44)$$

The side bands of $\hat{\mathbf{M}}$ are proportional to the Fourier components of δr . After a normalization of the main diagonal $\hat{\mathbf{D}}^{-1}\hat{\mathbf{M}}$ the matrix is diagonal dominant if

$$\left| F_{m-n} \{\delta r\} \frac{k_1 J_1(k_{r,n}R_0)}{k_{r,n} J_0(k_{r,n}R_0)} ((m+n)k_0 + nm k_1) \right| \ll 1,$$

(for simplicity the terms proportional to Z_s are neglected). This is usually the case for shallow corrugations, low order expansions and frequencies with $J_0(k_{r,n}R_0) \neq 0$, $|F_{m-n} \{\delta r\} k_0| \ll 1$. We use a 1st order approximation to invert the matrix:

$$\begin{aligned}
\hat{\mathbf{c}} &= -2\pi R_0 (\hat{\mathbf{D}} + \hat{\mathbf{W}})^{-1} \tilde{\mathbf{v}} \approx -2\pi R_0 (\hat{\mathbf{D}}^{-1} - \hat{\mathbf{D}}^{-1} \hat{\mathbf{W}} \hat{\mathbf{D}}^{-1}) \tilde{\mathbf{v}} \\
\hat{\mathbf{C}}_0 &= -2\pi R_0 (\tilde{\mathbf{v}})_{N+1} - 2\pi \sum_{k=1}^{2N+1} (\hat{\mathbf{D}}^{-1} \hat{\mathbf{W}})_{N+1,k} (\hat{\mathbf{D}}^{-1} \tilde{\mathbf{v}})_k
\end{aligned} \quad . \quad (45)$$

As the vector $\tilde{\mathbf{v}}$ scales with the Fourier components of δr the result is a 2nd order approximation (with respect to δr). The equivalent surface impedance follows from Eq. (23a) as

$$Z_s(j\omega) = Z_b - \frac{1}{j\omega\epsilon_0} \sum_{n=-N}^N \frac{X_{0,n} |F_n \{\delta r\}|^2 (nk_1 k_0 - j\omega\epsilon_0 Z_b / R_0)}{J_0(k_{r,n}R_0) + j\omega\epsilon_0 Z_b J_1(k_{r,n}R_0) / k_m}. \quad (46)$$

The beam impedance calculated by Eqs. (22b,46) is denoted as **LB-N,2nd approximation**. For sinusoidal corrugations with PEC boundary conditions it is identical to the LB-1 approximation (which was derived with an exact matrix inversion).

As the LB-N,2nd approximation is a linear function of the squared Fourier amplitudes $|F_n \{\delta r\}|^2$ of the surface function, we can find another formulation that depends on the spectral power density $S_c(k)$ of δr . The autocorrelation function and the spectral power density are defined by:

$$R_c(s) = \lim_{S \rightarrow \infty} \frac{1}{S} \int_{-S}^S \delta r(x) \delta r(x-s) dx, \quad (47a)$$

$$S_c(k) = \int_{-\infty}^{\infty} R_c(s) \exp(-jks) ds. \quad (47b)$$

$\sqrt{R_c(0)}$ is the rms value of δr and $S_c(0) = 0$ because the mean value of the surface function δr vanishes. The spectral power density of a periodic surface function is a series of dirac pulses:

$$S_c(k) = 2\pi \sum_n F_n(\delta r) \delta(k - nk_1). \quad (48)$$

Only terms with $|n| \leq N$ are taken into account by the LB- $N, 2^{\text{nd}}$ approximation. The equivalent surface impedance can be expressed by an integral

$$Z_s(\omega) = Z_b + \frac{1}{2\pi} \int_{-\infty}^{\infty} S_c(\omega) Z_k(\omega, k) ds, \quad (49)$$

with the kernel

$$Z_k(\omega, k) = jk_0 Z_0 \frac{\left(j \frac{Z_b}{Z_0} J_0 + \frac{J_1}{k_r} \left(k - \frac{j Z_b}{R_0 Z_0} \right) \right) \left(k - \frac{j Z_b}{R_0 Z_0} \right)}{J_0 + jk_0 \frac{Z_b J_1}{Z_0 k_r}}, \quad (50)$$

$$k_r = \sqrt{k_0^2 - (k_0 + k)^2}, \quad J_0 = J_0(k_r R_0), \quad J_1 = J_1(k_r R_0).$$

As the side bands of the matrix $\tilde{\mathbf{M}}$ (Eq. (19)) are also proportional to the Fourier components of δr one can use a similar method to approximate $\tilde{\mathbf{M}}^{-1}$ and to obtain directly a 2^{nd} order approximation of the beam impedance. The result is $-1/2\pi R_0$ times the equivalent surface impedance given by Eq. (46). This direct approximation is less accurate than the LB- $N, 2^{\text{nd}}$ approximation: e.g. the resonances found by the LB-1 method are not estimated sufficiently and the sum of loss-parameters $\sum k_n$ diverges. There are two reasons why the method with the equivalent surface impedance produces better results: $\hat{\mathbf{M}}$ fulfills the diagonal dominance better than $\tilde{\mathbf{M}}$ although these matrices differ only in column N , and $\tilde{\mathbf{M}}$ is singular at the poles of Z_{beam} . Therefore the 1^{st} order inversion of $\tilde{\mathbf{M}}$ is in principle not possible at the pole frequencies, but the 1^{st} order inversion of $\hat{\mathbf{M}}$ can be possible because Z_s is finite at these frequencies. E.g. the LB- $N, 2^{\text{nd}}$ approximation is identical to the LB-1 approximation of a sinusoidal corrugation with PEC boundary.

For one example the LB- $N, 2^{\text{nd}}$ method is compared with the RMS-9 and LB-9 method. The wake potential of a gaussian bunch with $\sigma = 25\mu\text{m}$ is calculated for an aluminum beam pipe with the radius $R = 5\text{mm}$ and the surface function $\delta r(z) = 0.6\mu\text{m} \cos(2\pi z/60\mu\text{m}) \pm 0.18\mu\text{m} \cos(2\pi z/20\mu\text{m})$. For all methods and for both signs in the δr -function the wakes are almost plotted along the same curve, see Fig. 15. The deviation between the RMS-9 calculations with different sign in the δr -function is less than $7 \cdot 10^{10} \text{ V/(Cm)}$. For these parameters the LB- $N, 2^{\text{nd}}$ method is quite sufficient, but not the direct superposition of the wakes of sinusoidal PEC surfaces and the resistive wall wake. The deviation of the direct superposition to the RMS-9 approximation is of the order of $4 \cdot 10^{13} \text{ V/(Cm)}$.

2.7. Higher Order Effects

Higher order approximations (RMS- N , Fourier- N and LB- N with $N > 1$) find resonances of the beam impedance for frequencies above $2f_\lambda$ (with $f_\lambda := c_0/2\lambda$) which are not observed by $N = 1$ approximations or by the LB- N , 2nd method. Such very sharp resonances can be seen in Fig. 16 with the beam impedance in a narrow frequency range around $2f_\lambda$ of a pipe with sinusoidal corrugation. In this figure we can distinguish broad resonances (at $1.99135f_\lambda, 2.0013f_\lambda$) which are calculated even by the LB-1 method and sharp resonances (at $1.99997f_\lambda, 2.00003f_\lambda, 2.00008f_\lambda, 2.00016f_\lambda, \dots$) which are seen only by the higher order method. These resonances are related to poles of the equivalent surface impedance with a strength proportional to a^2 (the broad resonances) and a^4 (the sharp resonances), with a the amplitude of the sinusoidal corrugation. At higher frequencies above nf_λ appear further poles with a strength proportional to a^{2n} .

A comparison of wake potentials computed by the RMS-5 and LB-1 method for a period length $\lambda = 50 \mu\text{m}$ and a gaussian bunch with $\sigma = 6 \mu\text{m}$ can be seen in Fig. 17. For this example f_λ is approximately 38% of the rms frequency of the bunch spectrum. Therefore higher order resonances can be excited. Nevertheless the wakes calculated by both methods differ by less than $1.2 \cdot 10^{12} \text{ V}/(\text{Cm})$. For this example the contribution of the loss-parameters of the higher order resonances is negligible.

3. More Examples

3.1. Comparison with MAFIA [8]

A completely different calculation method for wake potentials is the numerical field integration in time domain [8]. To avoid an extreme numerical effort for this method, the ratios λ/a , σ/a and R_0/a should not be too large. Therefore wake potentials are calculated for a PEC beam pipe with $R_0 = 5 \text{ mm}$, $\delta r(z) = 10 \mu\text{m} \cos(2\pi z/1\text{mm})$ and gaussian bunches with the rms lengths $\sigma = 250 \mu\text{m}$, $\lambda = 1\text{mm}$. They are compared in Fig. 18 and 19 with wake potentials calculated by the LB-1 method.

3.2. Corrugation Wavelength

The wake potential of a gaussian bunch with the rms length $\sigma = 25 \mu\text{m}$ in a PEC beam pipe with the radius $R_0 = 5 \text{ mm}$ can be seen in Fig. 20 for different sinusoidal corrugations $\delta r(z) = a \cos(2\pi z/\lambda)$ with $a/\lambda = 0.02$ and $\lambda = 3, 6, 12, 25, 50, 100, 200 \mu\text{m}$. The wake is normalized to $a^2/(R\sigma^2\lambda\epsilon_0)$. In the given parameter range the normalized wake is of the order $0.1 \cdot a^2/(R\sigma^2\lambda\epsilon_0)$. The shape changes from inductive for small values of λ to resonant for $\lambda \approx \sigma$. The wake has its largest magnitude if the corrugation wavelength is approximately equal to the rms bunch length. For larger corrugation wavelengths, multiple resonances of the beam impedance are excited. As these resonances are very dense they have a similar effect to a continuous spectrum: they cause a decaying contribution to the short range wake. Only the very first resonance can be isolated and contributes to the wake with an undamped oscillation.

4. TESLA FEL Beam Pipe

The measured surface structure [6] of a $720 \times 720 \mu\text{m}$ sample of a steel pipe can be seen in Fig. 21 as grayscale picture. The x, y, z coordinate system is cartesian with x perpendicular to the surface and z parallel to the beam axis. The resolution in x, z direction is $1.4 \mu\text{m}$. The scaling of the x -axis can be seen in Fig. 22 with the two cuts $\delta x(0, z)$, $\delta x(y, 0)$. The strongest contribution to δx comes from the curvature of the pipe (y -direction) and a tilt in z -direction. Therefore we extract the curvature and tilt to get the surface function $\delta r(y, z) = \delta x(y, z) - (q_0 + q_y y + q_{y2} y^2 + q_z z)$. The parameters q_0, q_y, q_{y2}, q_z are chosen so that the mean value of δr is zero and the rms value is minimal. The grayscale picture of δr can be seen in Fig. 23 and two 1D plots with $\delta r(0, z)$, $\delta r(y, 0)$ are shown in Fig. 24. The y -axis corresponds to the azimuthal φ coordinate. The 2D autocorrelation function (ACF) is calculated by

$$R_{c,2D}(y, z) = \frac{1}{A(y, z)} \int_{A(y, z)} \delta r(\hat{y}, \hat{z}) \delta r(\hat{y} - y, \hat{z} - z) d\hat{y} d\hat{z}.$$

Due to the limited sample size the integration area $A(y, z)$ depends on the arguments of the ACF. For large distances $\sqrt{y^2 + z^2}$ from the origin, A is small and $R_{c,2D}$ uncertain. Therefore the domain of the grayscale picture of $R_{c,2D}(y, z)$ in Fig. 25 is limited to points with $\sqrt{y^2 + z^2} \leq 500 \mu\text{m}$. The amplitude of $R_{c,2D}$ can be seen in Fig. 26 with a 1D cut of $R_{c,2D}$ along the z -axis. The square root at the origin is the rms value of the roughness $\delta r_{\text{rms}} = \sqrt{R_{c,2D}(0, 0)} = 0.58 \mu\text{m}$. As the theory of this report is developed for axially symmetric structures we use $R_{c,2D}(0, z)$ instead of the 1D ACF $R_c(z)$ defined by Eq. (47a). For simplicity we write $R_c(z) = R_{c,2D}(0, z)$. As $R_c(z)$ is also uncertain for larger arguments we use three types of extrapolation, which are plotted together with R_c in Fig. 26. These extrapolations start from $z = 500 \mu\text{m}$ (extrapolation 1), $z = 300 \mu\text{m}$ (extrapolation 2) and $z = 200 \mu\text{m}$ (extrapolation 3). The extrapolation functions are chosen so that the mean value of the ACF vanishes. The spectral power density $S_c(k)$ is calculated by Eq. (47b). The integrated and normalized power density

$$IS(k) := \frac{1}{\delta r_{\text{rms}}^2} \int_{-k}^k S_c(K) dk$$

describes the fractional contribution of wave numbers below k to the total roughness (cf. Fig. 27). About 80% of $\delta r_{\text{rms}}^2 = R_c(0)$ is caused by the spectrum below $k = 2.6 \cdot 10^4 \text{ m}^{-1}$ or by wavelengths larger than $\lambda = 240 \mu\text{m}$, only 10% of δr_{rms}^2 is caused by the spectrum above $k = 4.7 \cdot 10^4 \text{ m}^{-1}$ or by wavelengths shorter than $\lambda = 134 \mu\text{m}$. This means a bunch with the rms length $\sigma = 25 \mu\text{m}$ is not short compared to the typical wavelength of the surface structure. On the other side one may doubt that the sample size of $720 \times 720 \mu\text{m}$ is large enough to obtain a significant surface description. To see the effect of the arbitrary extrapolation of the ACF we calculate the wake potentials for all three extrapolations for a gaussian bunch with the rms length $\sigma = 25 \mu\text{m}$ in a copper plated beam pipe with different radii by the LB-

$N, 2^{\text{nd}}$ method. Figs. 28 and 29 show two results of such calculations together with the resistive wall wake of a pipe with perfect surface. As the curves for different extrapolations are almost identical we assume the wake potential is insensitive to the type of extrapolation. Some characteristic parameters of the wake potential (for extrapolation 3) are summarized in the following tables:

resistive (cu) gaussian bunch	$\min(W^\sigma)$ V/pCm	$\max(W^\sigma)$ V/pCm	$\langle W^\sigma \rangle$ V/pCm	$\text{rms}(W^\sigma)$ V/pCm
$R_0 = 3\text{ mm}$	-111	54.1	-44.9	56.7
$R_0 = 4\text{ mm}$	-85.7	43.4	-34.9	44.1
$R_0 = 5\text{ mm}$	-70.3	38.0	-29.0	36.5
$R_0 = 6\text{ mm}$	-59.8	34.8	-25.2	31.3

resistive+rough gaussian bunch	$\min(W^\sigma)$ V/pCm	$\max(W^\sigma)$ V/pCm	$\langle W^\sigma \rangle$ V/pCm	$\text{rms}(W^\sigma)$ V/pCm
$R_0 = 3\text{ mm}$	-129	69.6	-47.9	68.7
$R_0 = 4\text{ mm}$	-99.7	58.2	-37.7	54.0
$R_0 = 5\text{ mm}$	-82.0	52.6	-31.7	45.1
$R_0 = 6\text{ mm}$	-69.8	48.8	-27.9	38.7

Similar calculations are done for a more rectangular bunch. The precise bunch shape is calculated as the convolution $\lambda_{\text{rect}}^\sigma(s) = \lambda_{\text{rect}}^\sigma(s) \otimes (g(s/\sigma_2)/\sigma_2)$ of a rectangular distribution $\lambda_{\text{rect}}^\sigma(s) = 1/(2\sqrt{3}\sigma)$ for $|s| < \sqrt{3}\sigma$ and a gaussian distribution $g(x)$ with $\sigma = 25\mu\text{m}$ and $\sigma_2 = 3\mu\text{m}$. Again the results are almost identical for all extrapolations of the ACF. The bunch shape, the resistive wall wake and the wake in a pipe with rough surface are shown in Figs. 30 and 31 for beam pipes of different radii. The following tables list some characteristic parameters of the wake potential (for extrapolation 3):

resistive (cu) "rect." Bunch	$\min(W^\sigma)$ V/pCm	$\max(W^\sigma)$ V/pCm	$\langle W^\sigma \rangle$ V/pCm	$\text{rms}(W^\sigma)$ V/pCm
$R_0 = 3\text{ mm}$	-235	219	-55.0	72.9
$R_0 = 4\text{ mm}$	-159	133	-40.7	50.9
$R_0 = 5\text{ mm}$	-117	98.7	-33.4	38.2
$R_0 = 6\text{ mm}$	-91.1	81.4	-28.7	29.8

resistive+rough “rect.” Bunch	$\min(W^\sigma)$ V/pCm	$\max(W^\sigma)$ V/pCm	$\langle W^\sigma \rangle$ V/pCm	$\text{rms}(W^\sigma)$ V/pCm
$R_0 = 3\text{ mm}$	-264	228	58.6	88.5
$R_0 = 4\text{ mm}$	-178	152	-45.2	62.0
$R_0 = 5\text{ mm}$	-131	124	-38.1	45.7
$R_0 = 6\text{ mm}$	-102	97.0	-32.0	35.8

5. Conclusion

Three different methods (RMS- N , Fourier- N , LB- N) have been developed to calculate the monopole impedance and wake potential in beam pipes with periodical, smooth, shallow corrugation and finite conductivity. The numerical effort determined by a linear equation system of the dimension $2N + 1$ and the number of frequency points which are needed for the inverse Fourier transformation. For all examples in this report a good convergence was achieved for $N < 10$ or even $N = 1$. The LB- N , 2nd method uses a first order approximation for the solution of the equation system. It is of 2nd order accuracy with respect to the impedance. This method is explicit. In this approximation, the contributions of different Fourier components of the surface structure to the equivalent surface impedance can be calculated independently from each other. For various examples low order calculations were found in good agreement with higher order calculations or with a time domain computation method. Based on the statistical properties of a measured surface structure the wake fields in a copper plated undulator beam pipe have been investigated. For the investigated parameters the short range wake was increased by approximately 23% compared to a resistive pipe without roughness.

6. Acknowledgements

The author would like to express his thanks to J.Pflüger, M.Timm, A.Novokhatski, R.Brinkmann, J.Rosbach for many helpful and clarifying discussions and to S.Wipf for carefully reading the text.

References

- [1] K.L.F. Bane, C.K. Ng and A.W. Chao, SLAC-PUB-7514, May 1997.
- [2] G.V. Stupakov, Phys. Rev. ST-AB 1, 064401 (1998).
- [3] A.Novokhatski, M. Timm, T. Weiland. TESLA 99-17, Sept. 1999.
- [4] K.Bane,A.Novokhatski, The Resonator Impedance Model of Surface Roughness Applied to the LCLS Parameters, SLAC-AP-117, March 1999.
- [5] G.Stupakov, Surface Impedance and Synchronous Modes, SLAC-PUB-8202, July 1999.
- [6] U.Hahn, T.Rymarczyk, DESY-HASYLAB, private communications Sept. 2000;

- [7] R. Unbehauen: Synthese elektrischer Netzwerke, R.Oldenbourg Verlag München Wien, 1972.
- [8] The MAFIA Colaboration, CST GmbH, Buendinger Str. 2a, D-64289 Darmstadt, Germany.

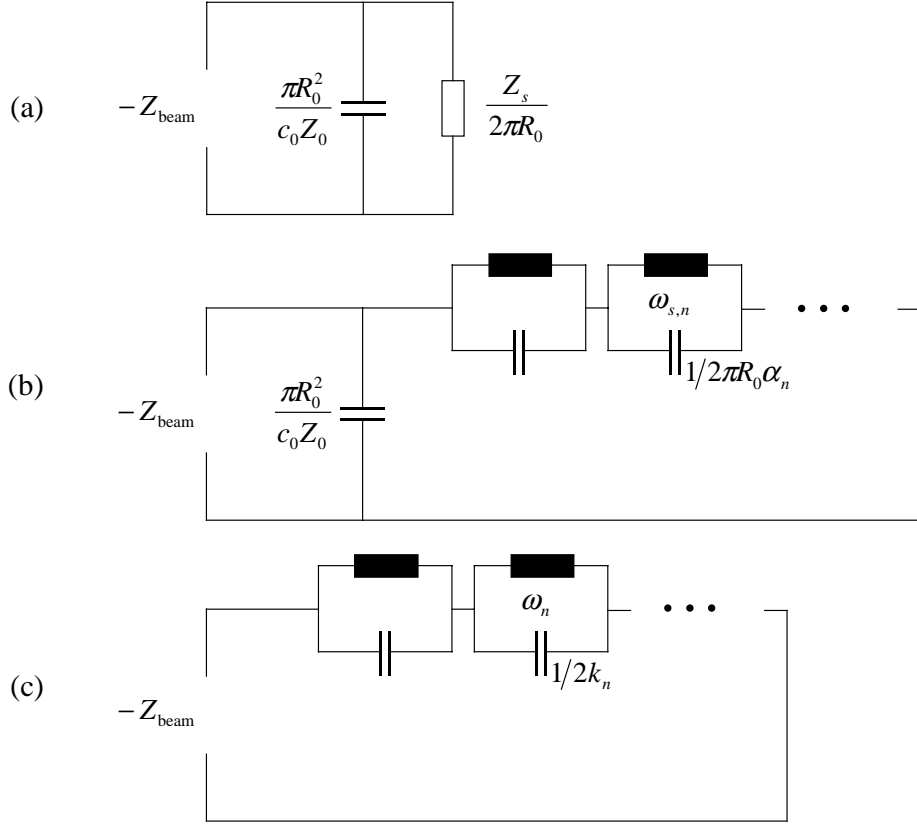


Fig. 1: Network description of the beam impedance and the equivalent surface impedance.

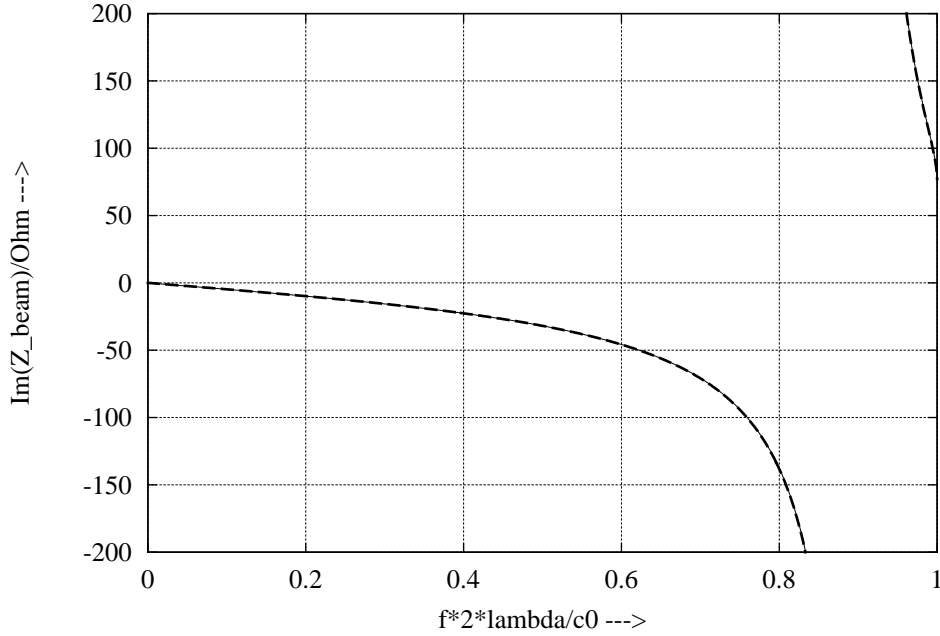


Fig. 2: Beam Impedance: comparison of the LB-1 approximation (solid line) and Eqs. (22b, 41) (dashed line). Configuration: PEC pipe, $R_0 = 5 \text{ mm}$, $\delta r(z) = a \cos(2\pi z/\lambda)$, $a = 1 \mu\text{m}$, $\lambda = 50 \mu\text{m}$.

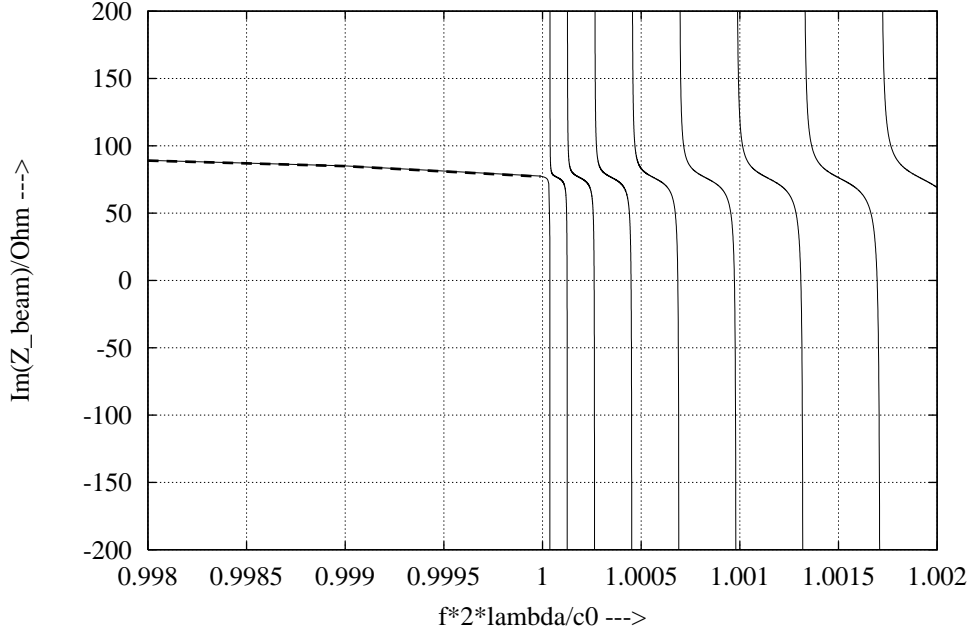


Fig. 3: The first higher resonances of the beam impedance: comparison of the LB-1 approximation (solid line) and Eqs. (22b, 41) (dashed line, only for $f2\lambda/c_0 < 1$). Configuration: same parameters as in Fig. 2.

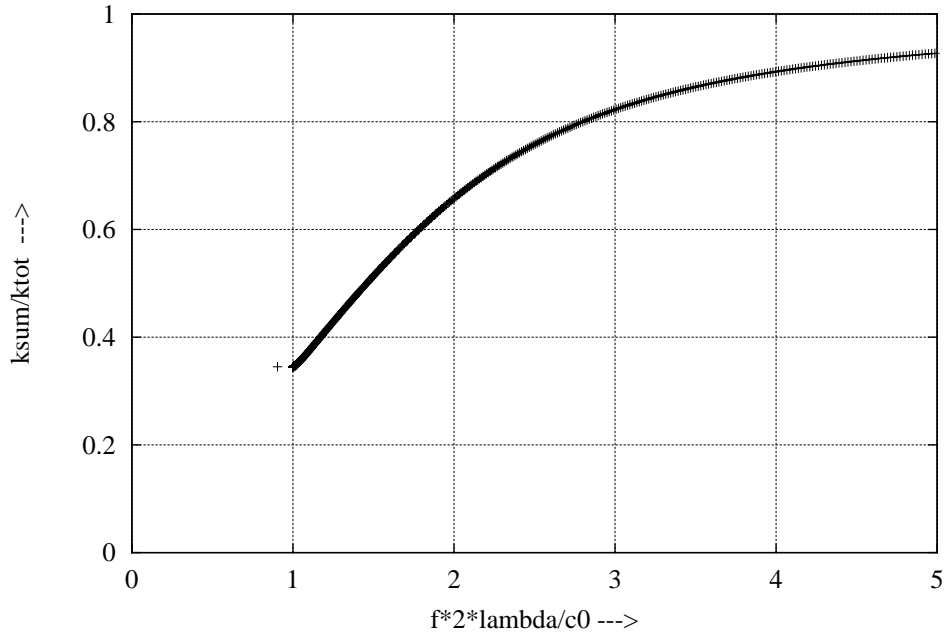


Fig. 4: Loss-parameter sum $K_n = \sum_{m=1}^n k_m$ as function of pole frequency ω_n for the LB-1 approximation. Configuration: same parameters as in Fig. 2.

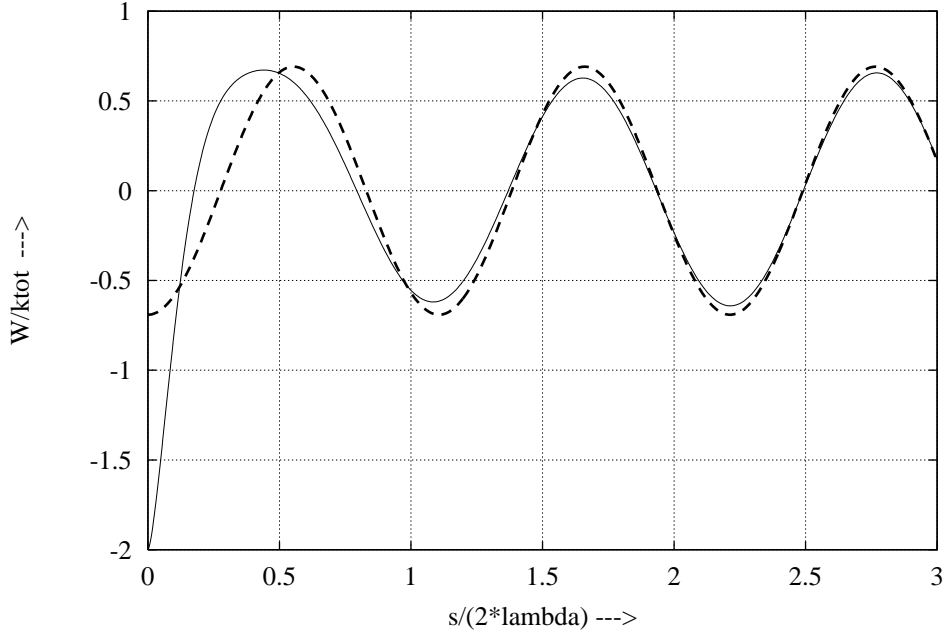


Fig. 5: Wake function calculated by the LB-1 approximation (solid line), contribution of the first resonance (dashed line). Configuration: same parameters as in Fig. 2.

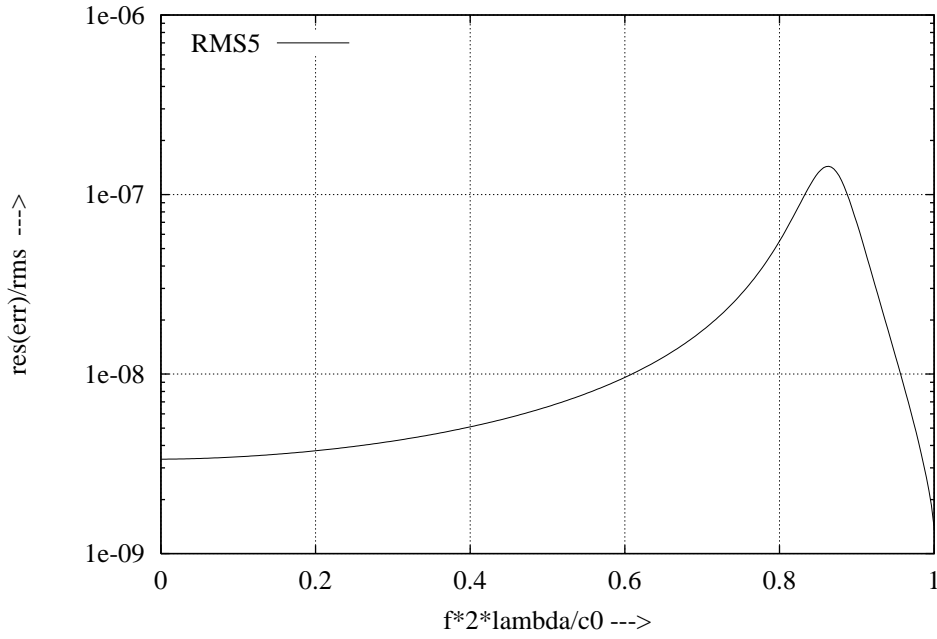


Fig. 6: Normalized boundary error $\|\mathbf{M}\mathbf{c} + \mathbf{v}\|/\|\mathbf{v}\|$ of the RMS-5 approximation. Configuration: same parameters as in Fig. 2, but with finite conductivity (aluminum).

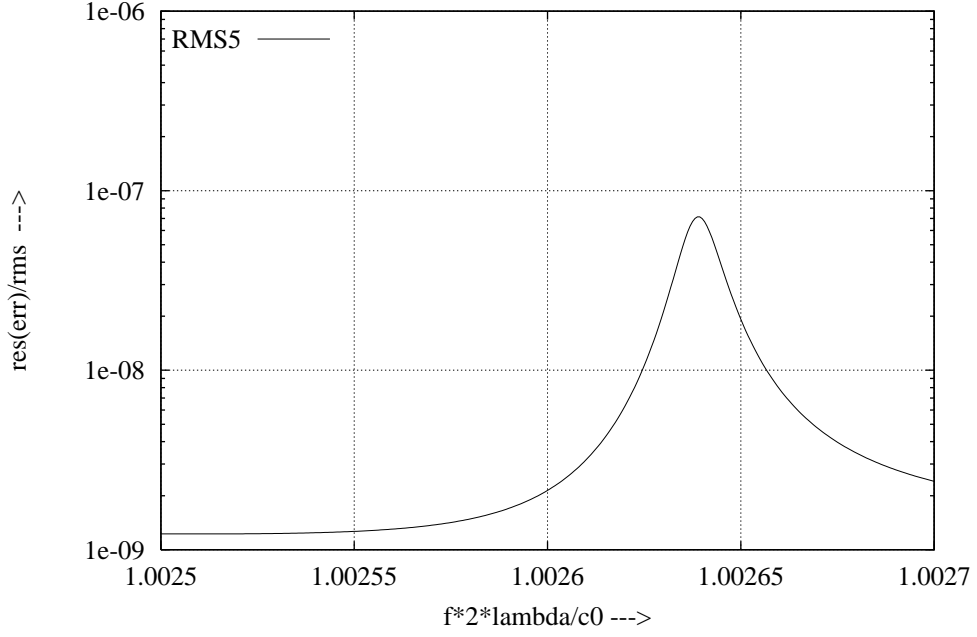


Fig. 7: Normalized boundary error $\|\mathbf{M}\mathbf{c} + \mathbf{v}\|/\|\mathbf{v}\|$ of the RMS-5 approximation for one of the first resonances above $c_0/2\lambda$. Configuration: same parameters as in Fig. 2, but with finite conductivity (aluminum).

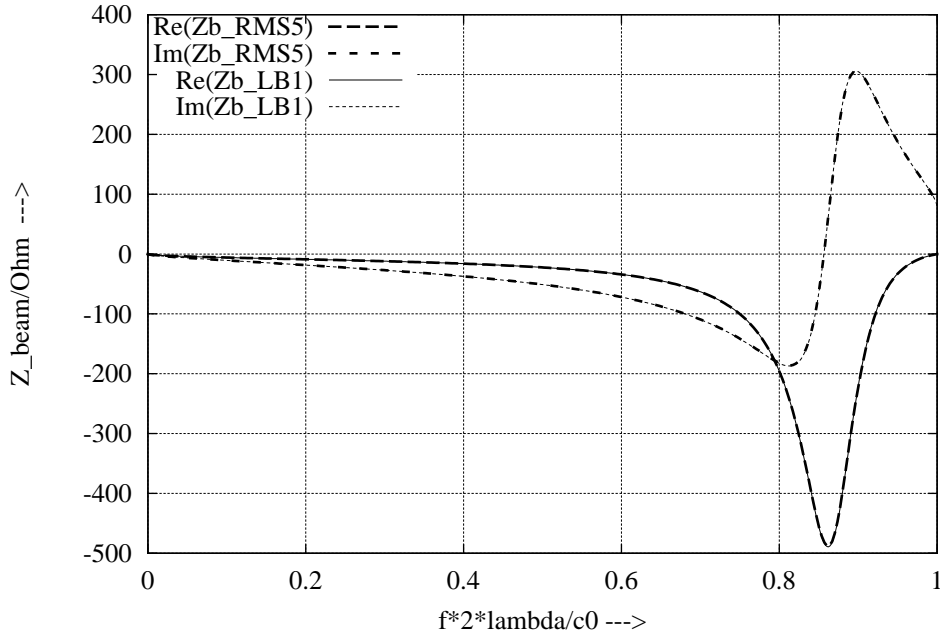


Fig. 8: Beam Impedance calculated by the RMS-5 and LB-1 approximation. Configuration: same parameters as in Fig. 2, but with finite conductivity (aluminum).

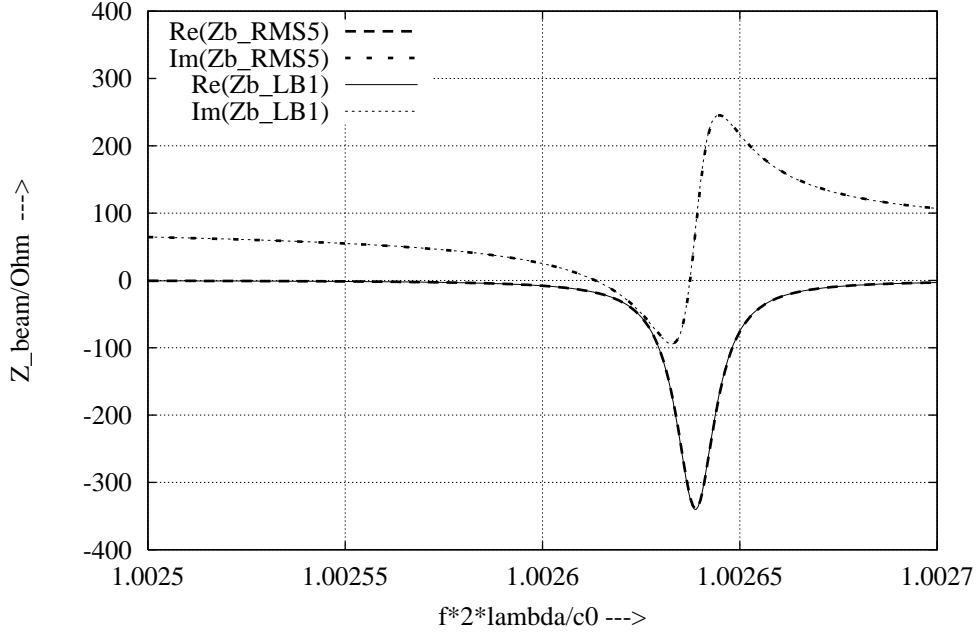


Fig. 9: Beam Impedance calculated by the RMS-5 and LB-1 approximation for one of the first resonances above $c_0/2\lambda$. Configuration: same parameters as in Fig. 2, but with finite conductivity (aluminum).

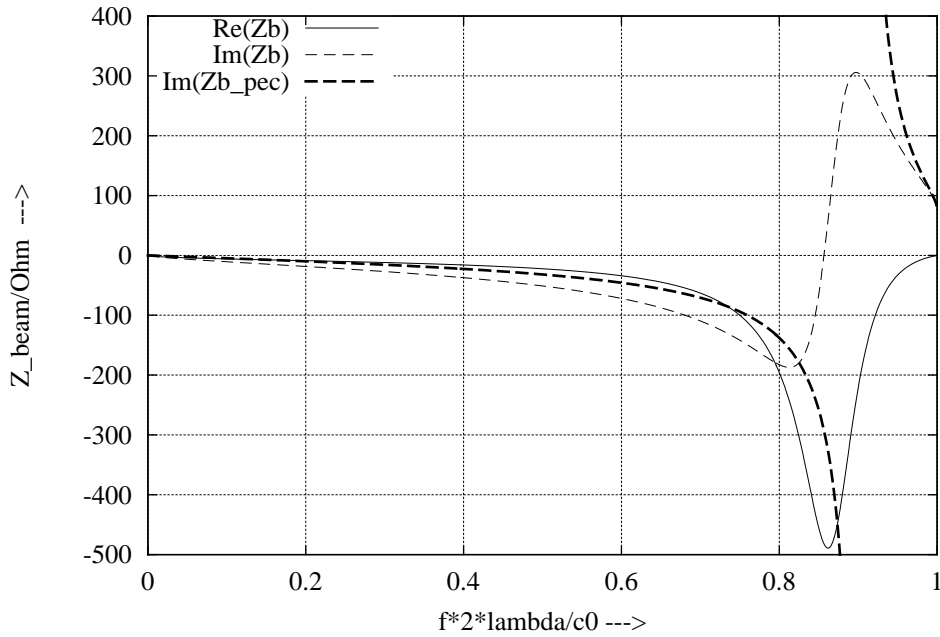


Fig. 10: Beam impedance calculated by the LB-1 approximation for perfect conductivity (imaginary part: thick dashed line) and finite conductivity (real part: solid line, imaginary part: dashed line). Configuration: same parameters as in Fig. 2, but with PEC boundary or finite conductivity (aluminum).

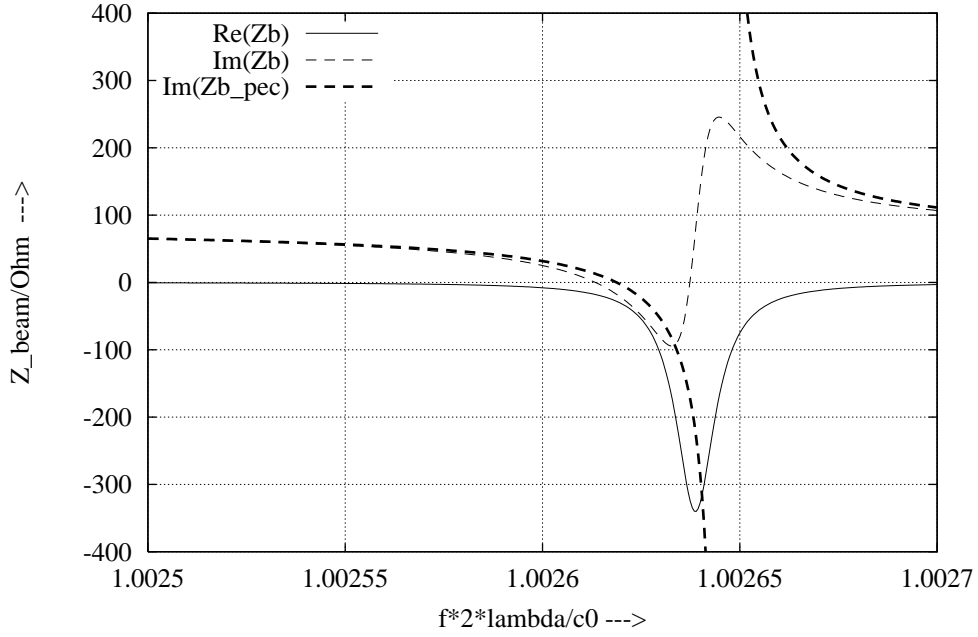


Fig. 11: One of the first resonances of the beam impedance above $c_0/2\lambda$ calculated by the LB-1 approximation: perfect conductivity (imaginary part: thick dashed line), finite conductivity (real part: solid line, imaginary part: dashed line). Configuration: same parameters as in Fig. 2, but with PEC boundary or finite conductivity (aluminum).

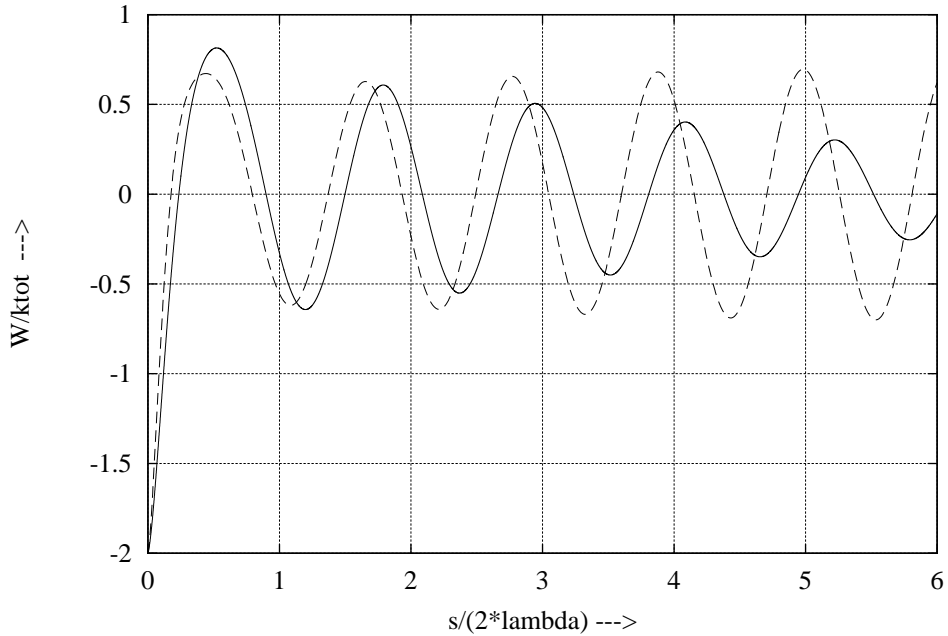


Fig. 12: Wake function calculated by the LB-1 approximation for perfect conductivity (solid line) and finite conductivity (dashed line). Configuration: same parameters as in Fig. 2, but with PEC boundary or finite conductivity (aluminum).

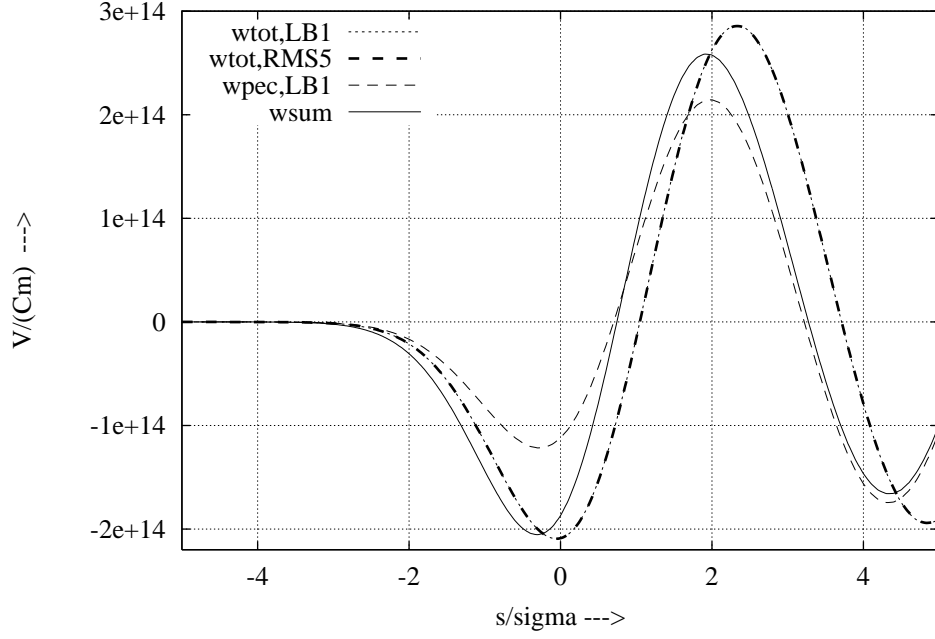


Fig. 13: Wake potential calculated by the LB-1 method (dotted line) and the RMS-5 method (thick dashed line) for a pipe with finite conductivity. Wake potential in a PEC pipe (LB-1, thin dashed line) and the sum of this wake and the resistive wall wake (solid line). Configuration: aluminum pipe, $R_0 = 5 \text{ mm}$, $\delta r(z) = a \cos(2\pi z/\lambda)$, $a = 1 \mu\text{m}$, $\lambda = 50 \mu\text{m}$, gaussian bunch with $\sigma = 25 \mu\text{m}$.

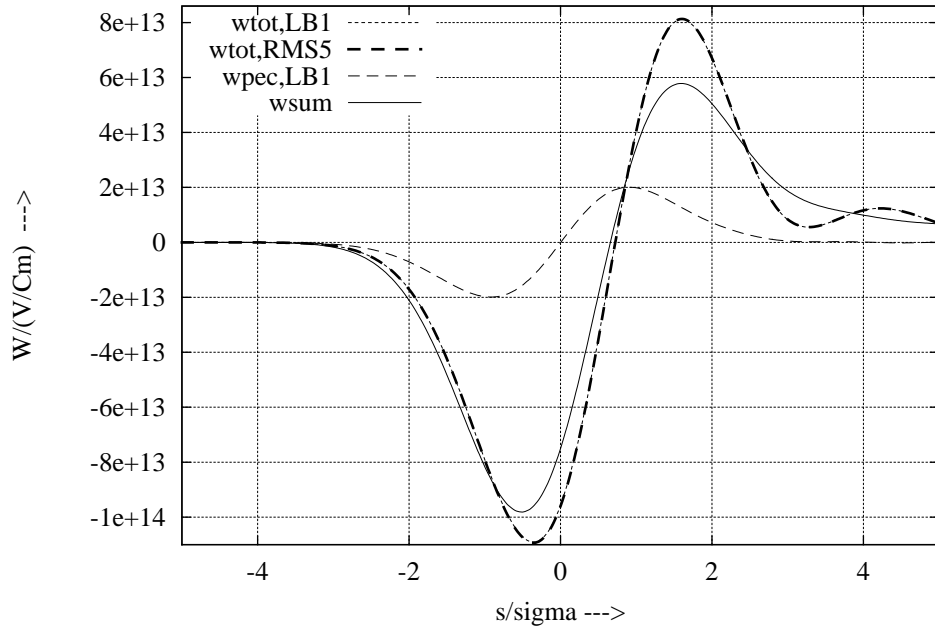


Fig. 14: Same curves as in Fig. 13 but for the configuration: aluminum pipe, $R_0 = 5 \text{ mm}$, $\delta r(z) = a \cos(2\pi z/\lambda)$, $a = 2 \mu\text{m}$, $\lambda = 10 \mu\text{m}$, gaussian bunch with $\sigma = 25 \mu\text{m}$.

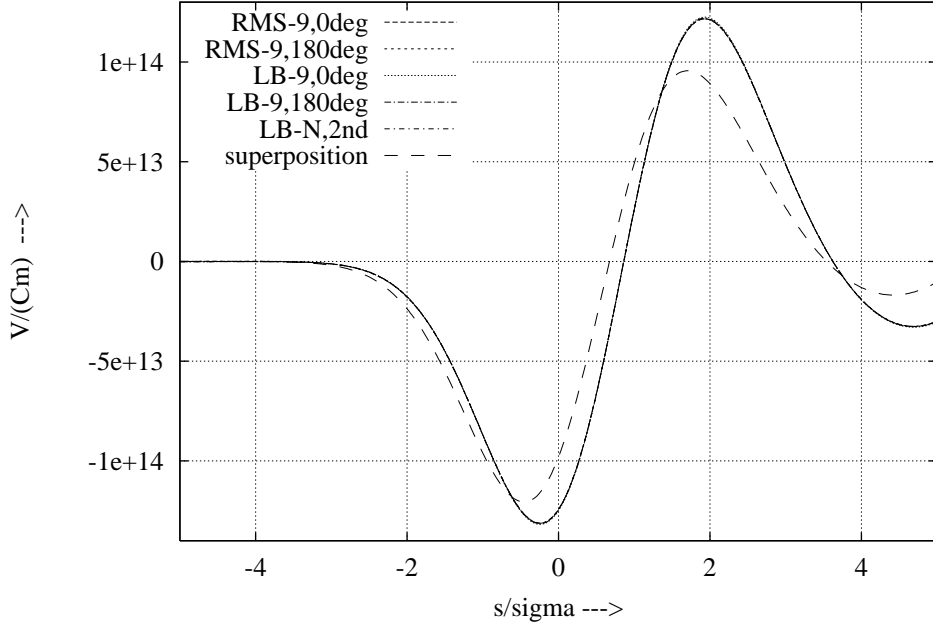


Fig. 15: Wake potential of a non-sinusoidal corrugation calculated by the RMS-9, LB-9 and LB- $N,2^{\text{nd}}$ method. All curves are plotted almost along the same line. The curves labeled with '0deg' and '180deg' correspond to the two signs in the δr -function. Superposition of the resistive wall wake and the PEC wakes of individual sinusoidal corrugations (dashed line). Configuration: aluminum pipe, $R = 5 \text{ mm}$, $\delta r(z) = 0.6 \mu\text{m} \cos(2\pi z/60 \mu\text{m}) \pm 0.18 \mu\text{m} \cos(2\pi z/20 \mu\text{m})$, gaussian bunch with $\sigma = 25 \mu\text{m}$.

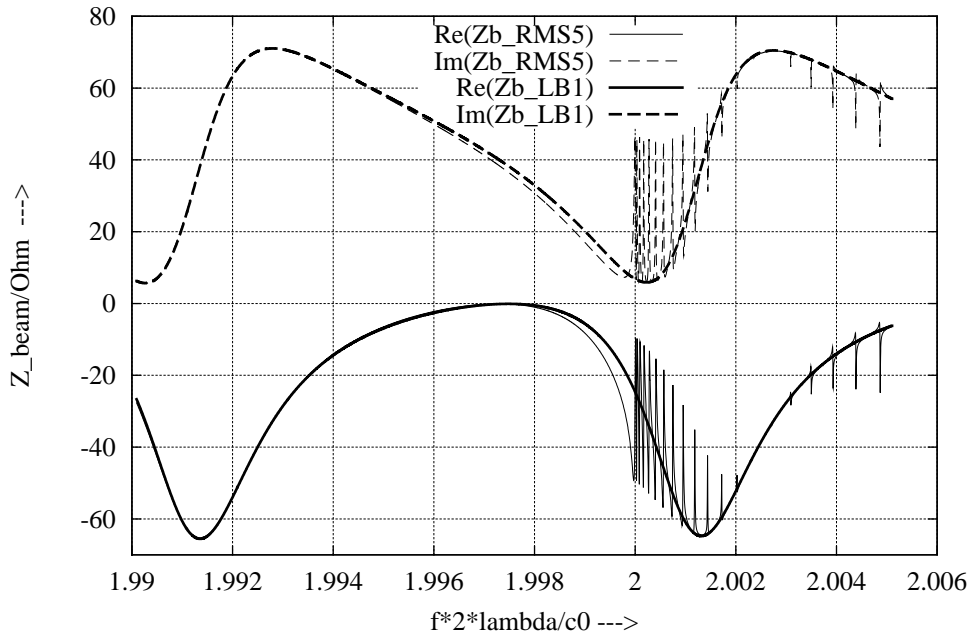


Fig. 16: Higher order effects: beam impedance calculated by the RMS-5 and LB-1 method. Configuration: same parameters as in Fig. 13.

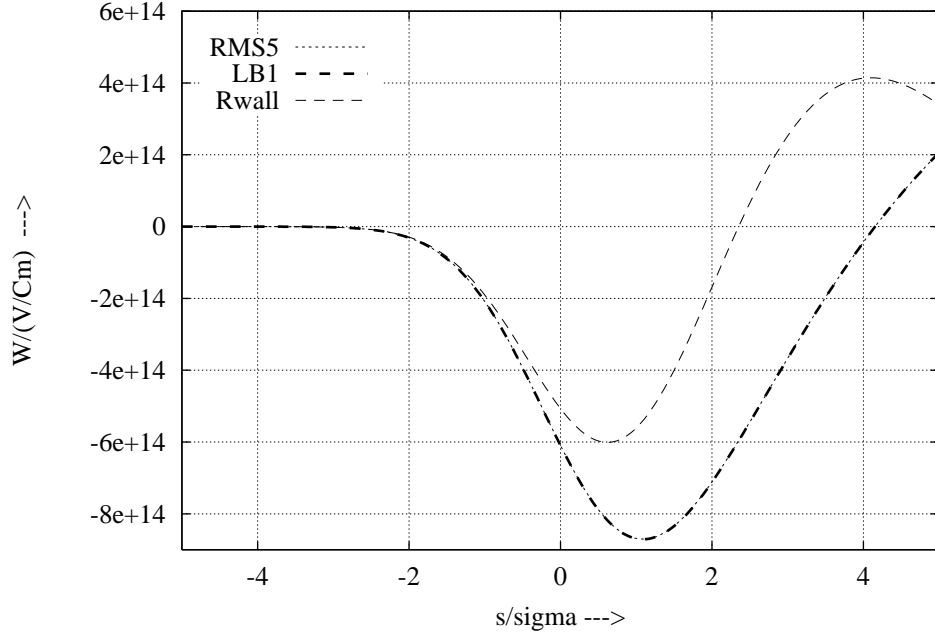


Fig. 17: Wake potential calculated by the RMS-5 and LB-1 method, resistive wall wake of a pipe without corrugation. Configuration: same parameters as in Fig. 13 but for a bunch with the rms length $\sigma = 6 \mu\text{m}$.

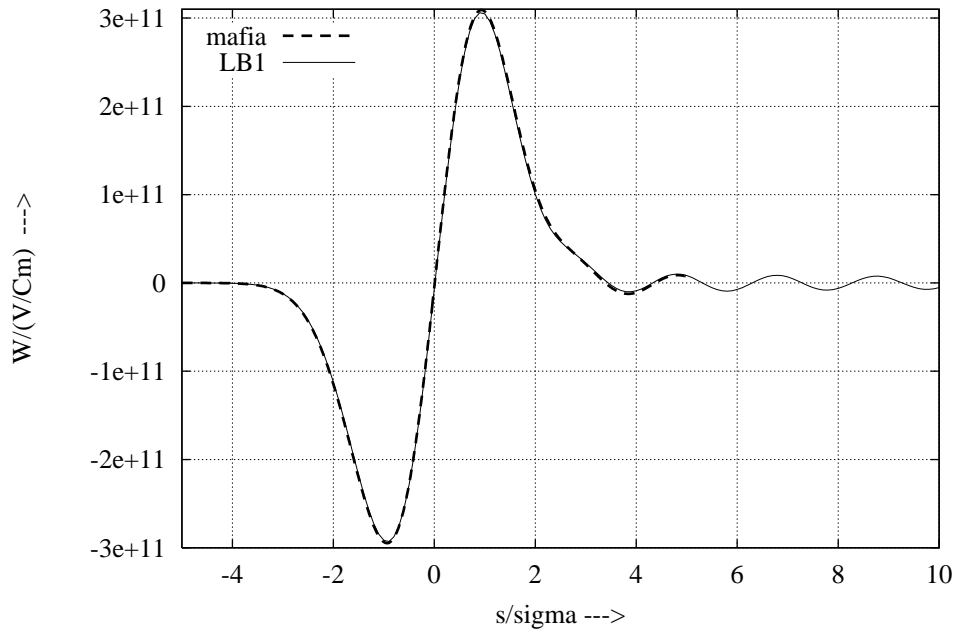


Fig. 18: Wake potential calculated by MAFIA and by the LB-1 method. Configuration: PEC pipe, $R_0 = 5 \text{ mm}$, $\delta r(z) = a \cos(2\pi z/\lambda)$, $a = 10 \mu\text{m}$, $\lambda = 1 \text{ mm}$, gaussian bunch with $\sigma = 1 \text{ mm}$.

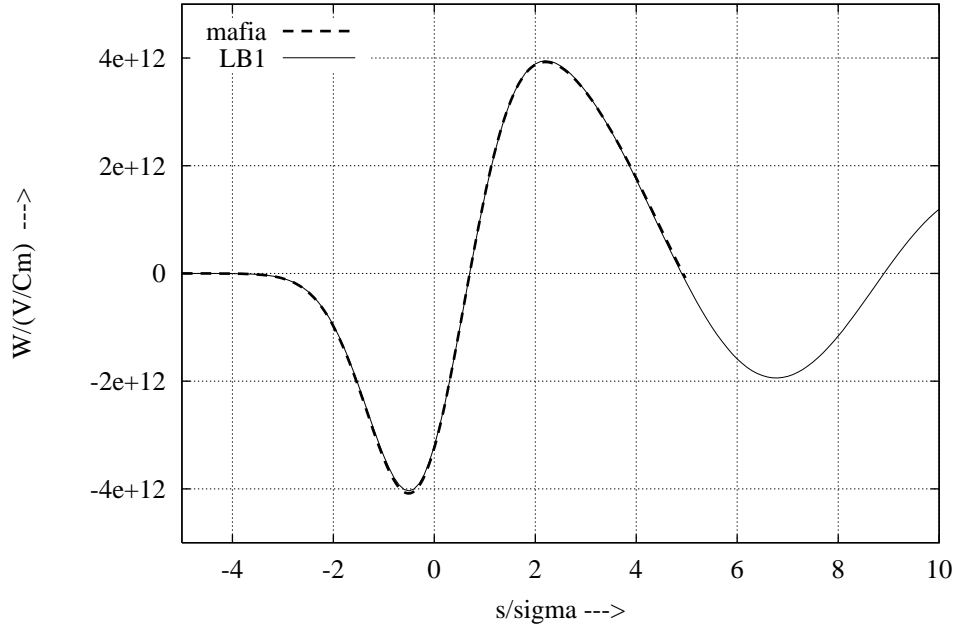


Fig. 19: Wake potential calculated by MAFIA and by the LB-1 method. Configuration: PEC pipe, $R_0 = 5 \text{ mm}$, $\delta r(z) = a \cos(2\pi z/\lambda)$, $a = 10 \mu\text{m}$, $\lambda = 1 \text{ mm}$, gaussian bunch with $\sigma = 250 \mu\text{m}$.

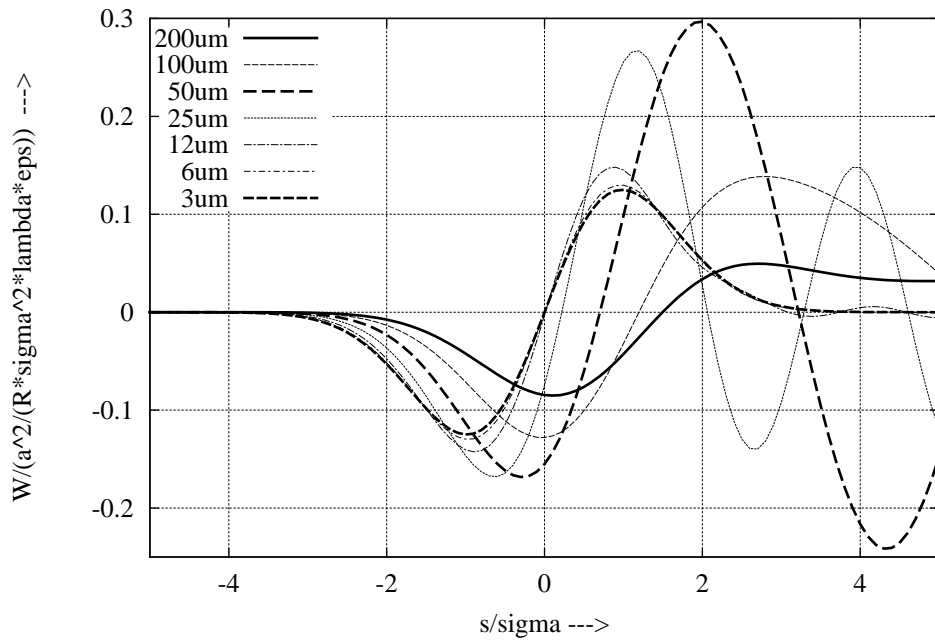


Fig. 20: Normalized wake potential of a pipe with various corrugation parameters calculated by the LB-1 method. The wake is normalized to $a^2/(R\sigma^2\lambda\epsilon_0)$. Configuration: PEC pipe, $R_0 = 5 \text{ mm}$, $\delta r(z) = a \cos(2\pi z/\lambda)$ with $a/\lambda = 0.02$ and $\lambda = 3, 6, 12, 25, 50, 100, 200 \mu\text{m}$.

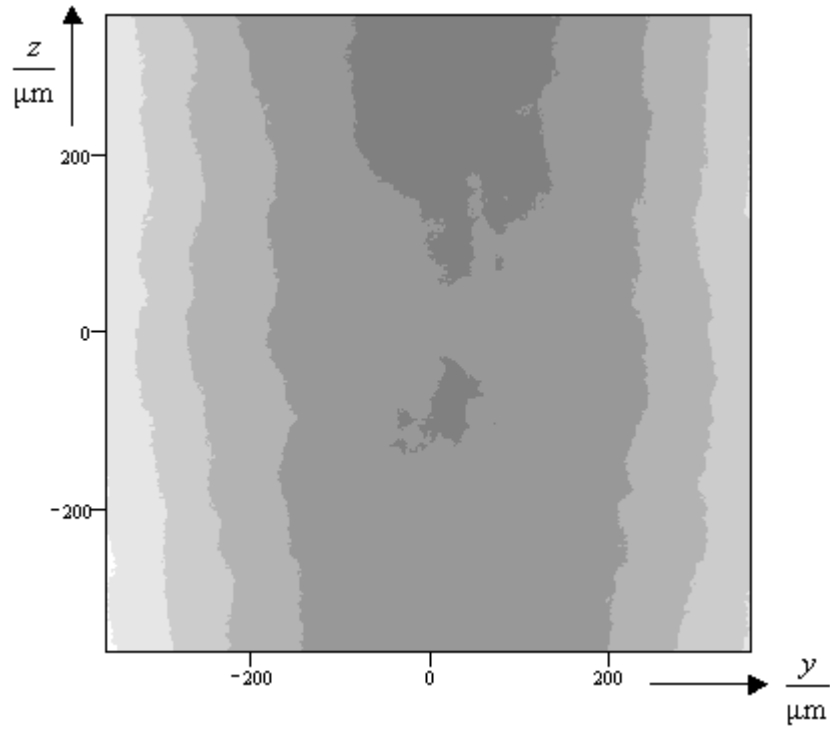


Fig. 21: Grayscale picture of a measured surface function $\delta x(y, z)$ [6]. The sample size is $720 \times 720 \mu\text{m}$, the resolution in y, z direction is $1.4 \mu\text{m}$. The gray scale ranges from 9 to $46 \mu\text{m}$.

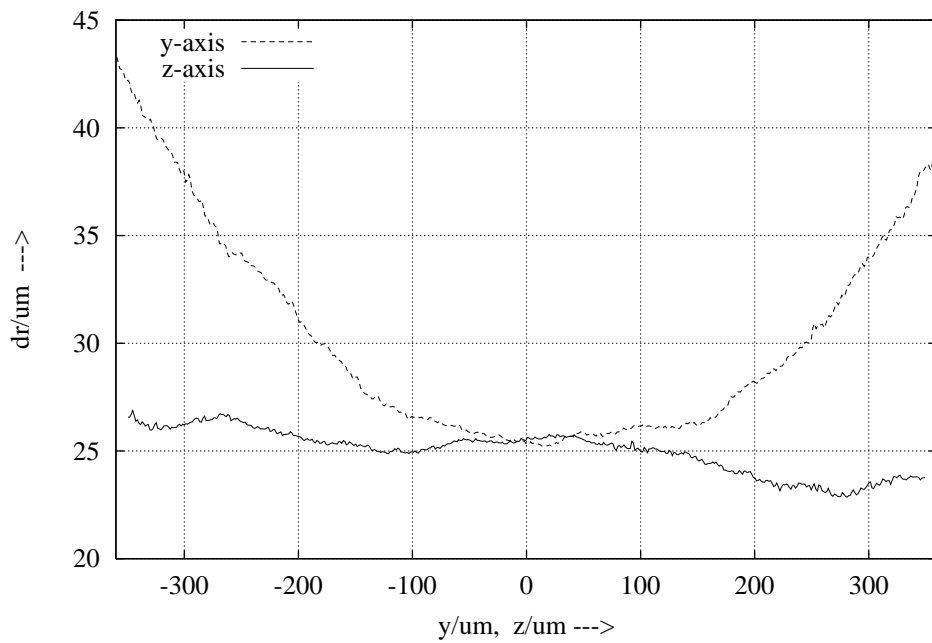


Fig. 22: 1D cuts $\delta x(0, z)$, $\delta x(y, 0)$ of the measured surface function in Fig. 21.

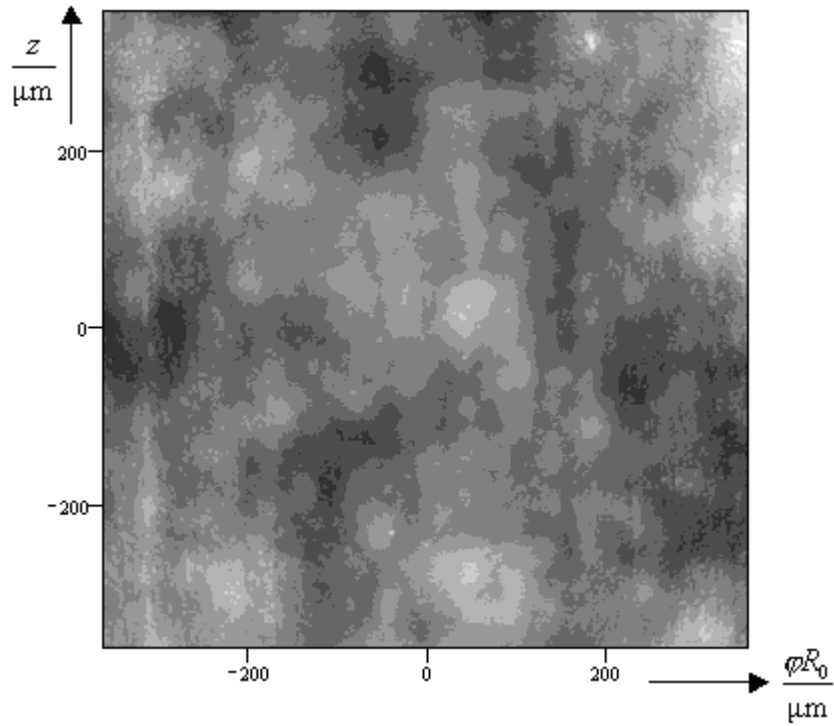


Fig. 23: Surface function $\delta r(y, z) = \delta x(y, z) - (q_0 + q_y y + q_{y2} y^2 + q_z z)$ after extraction of the curvature (in azimuthal direction) and slope (in z direction). The gray scale ranges from -2 to $2.8 \mu\text{m}$.

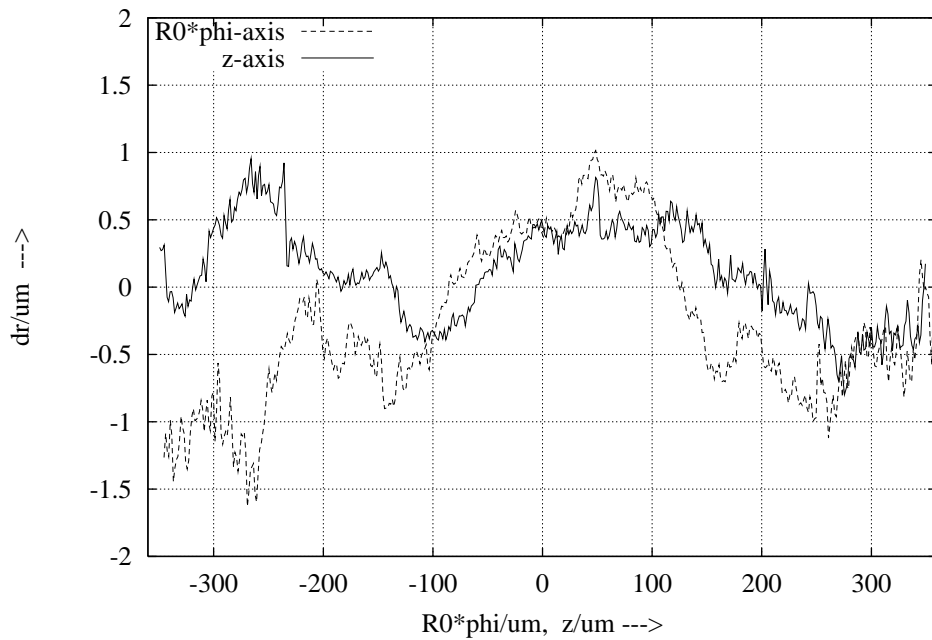


Fig. 24: 1D cuts $\delta r(0, z)$, $\delta r(y = R_0 \phi, 0)$ of the corrected surface function in Fig. 23.

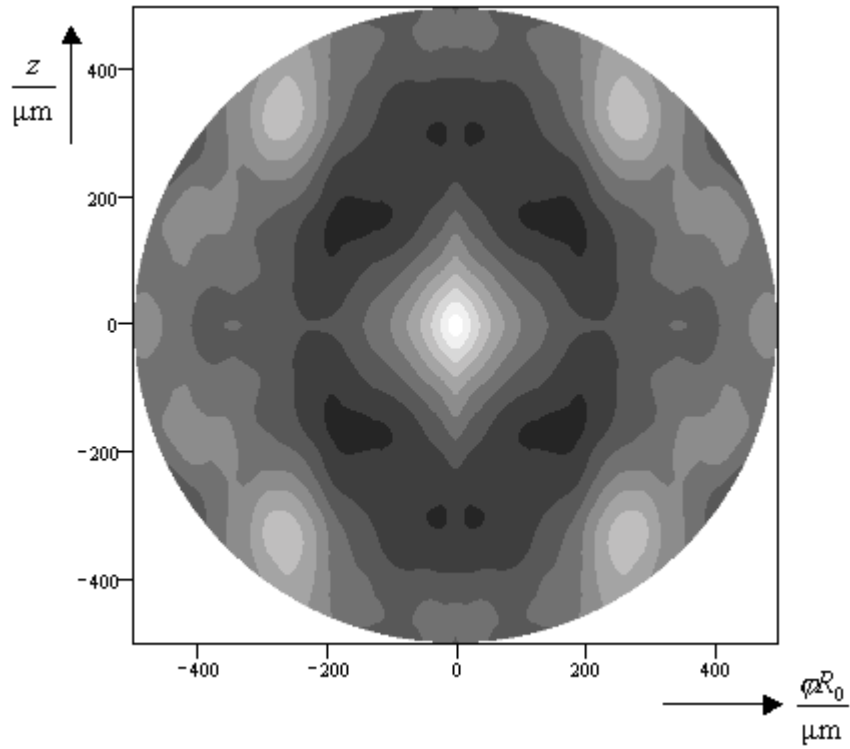


Fig. 25: 2D autocorrelation function $R_{c,2D}(y = R_0\phi, z)$ for points with $\sqrt{y^2 + z^2} \leq 500 \mu\text{m}$. The gray scale ranges from $-(0.34 \mu\text{m})^2$ to $(0.58 \mu\text{m})^2$.

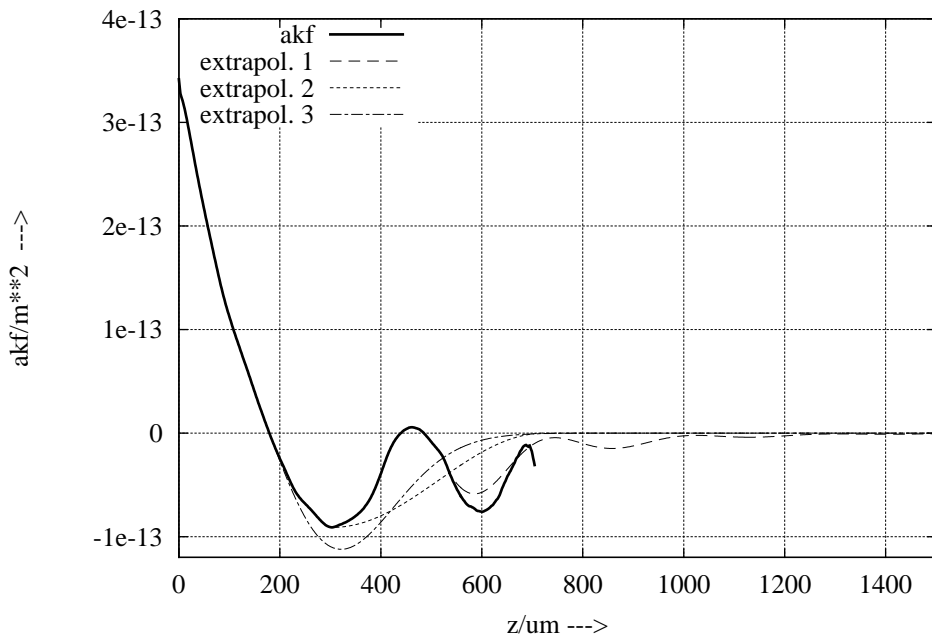


Fig. 26: 1D cut $R_c(z) = R_{c,2D}(0, z)$ of the ACF in Fig. 25 (thick line) and three different extrapolations for large arguments.

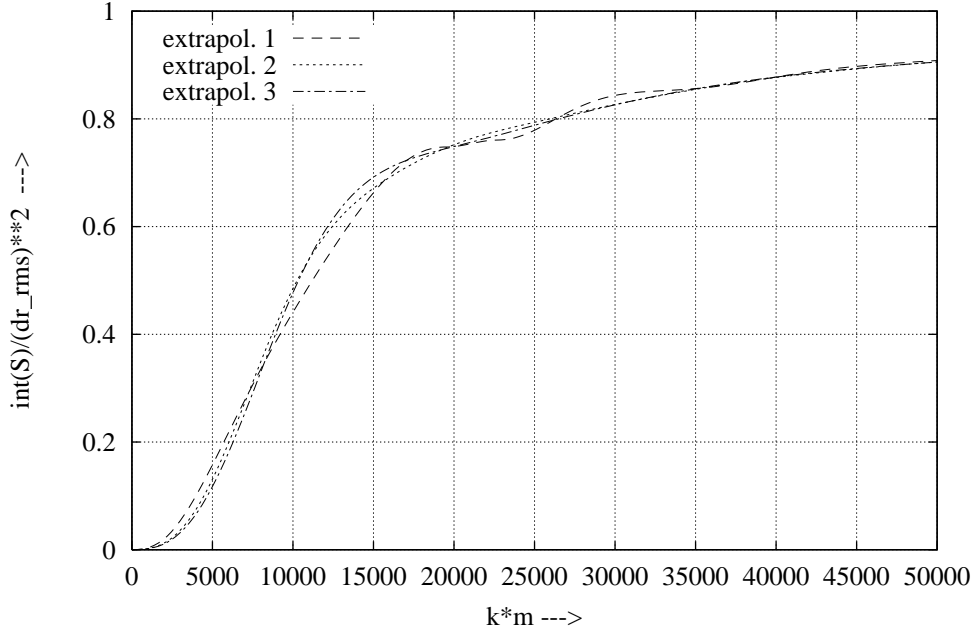


Fig. 27: Integrated normalized power density $IS(k) := \frac{1}{\sigma_{rms}^2} \int_{-k}^k S_c(K) dk$ calculated for the extrapolated ACF functions in Fig. 26.

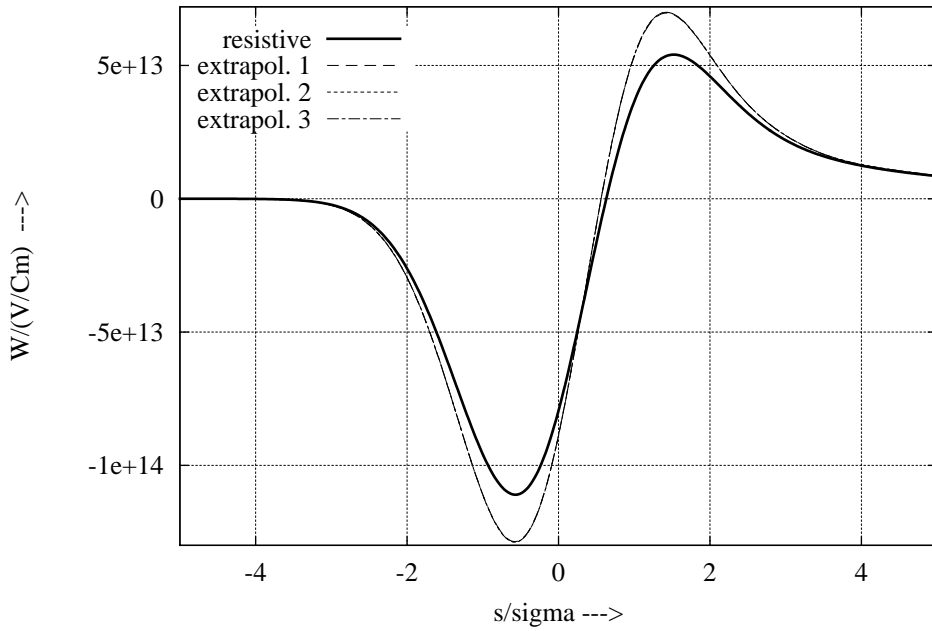


Fig. 28: Wake potential calculated by the LB-N,2nd method for three extrapolations of the ACF (thin lines), resistive wall wake (thick line) of a perfect pipe. Configuration: aluminum pipe, $R_0 = 3\text{mm}$, random surface, gaussian bunch with $\sigma = 25\ \mu\text{m}$.

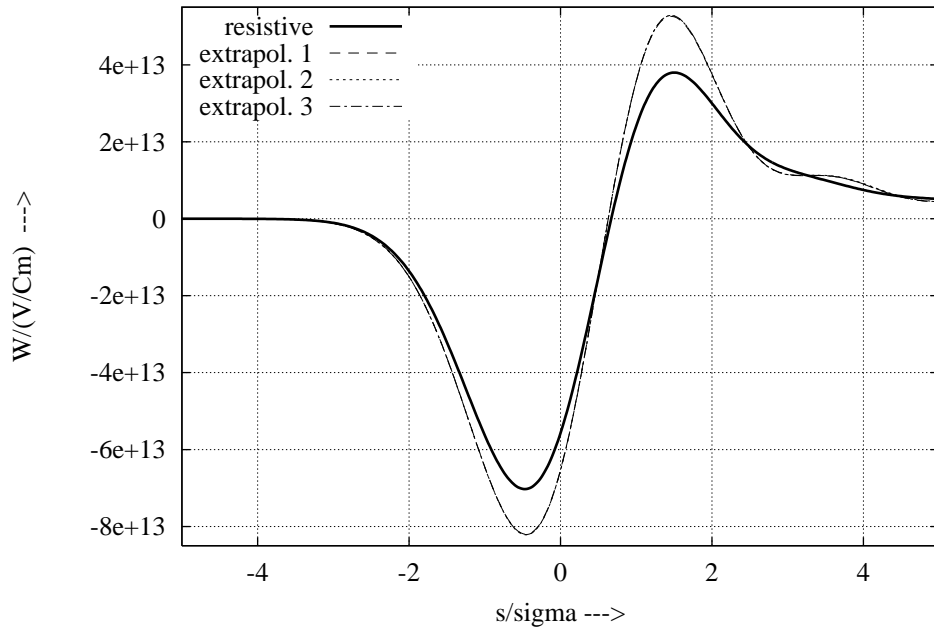


Fig. 29: Wake potential calculated by the LB-N,2nd method for three extrapolations of the ACF (thin lines), resistive wall wake (thick line) of a perfect pipe. Configuration: aluminum pipe, $R_0 = 5\text{ mm}$, random surface, gaussian bunch with $\sigma = 25\ \mu\text{m}$.

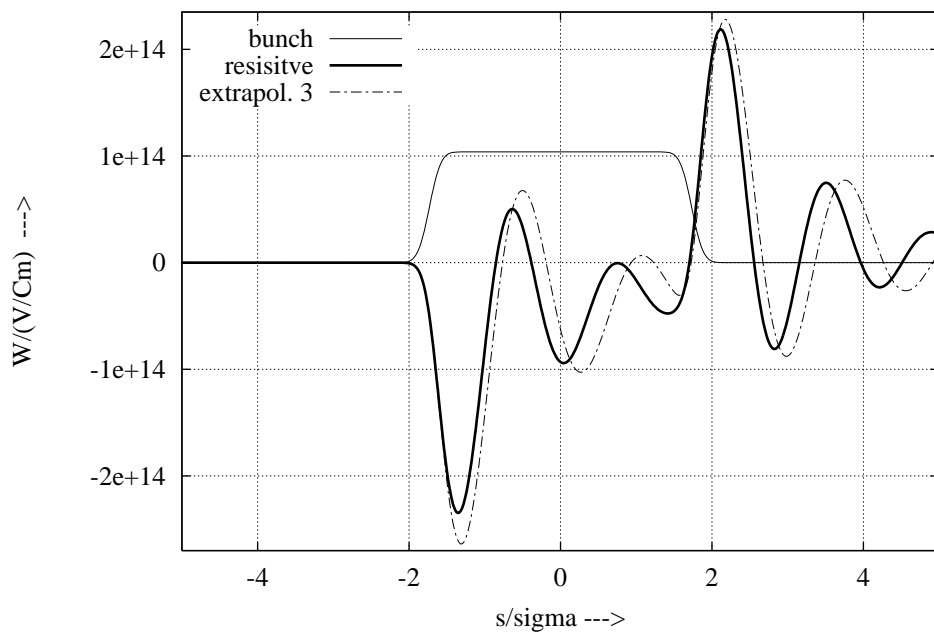


Fig. 30: Wake potential of a more rectangular bunch (solid line) calculated by the LB-N,2nd method (dot dashed line), resistive wall wake (thick line) of a perfect pipe. Configuration: aluminum pipe, $R_0 = 3\text{ mm}$, random surface, bunch shape see text.

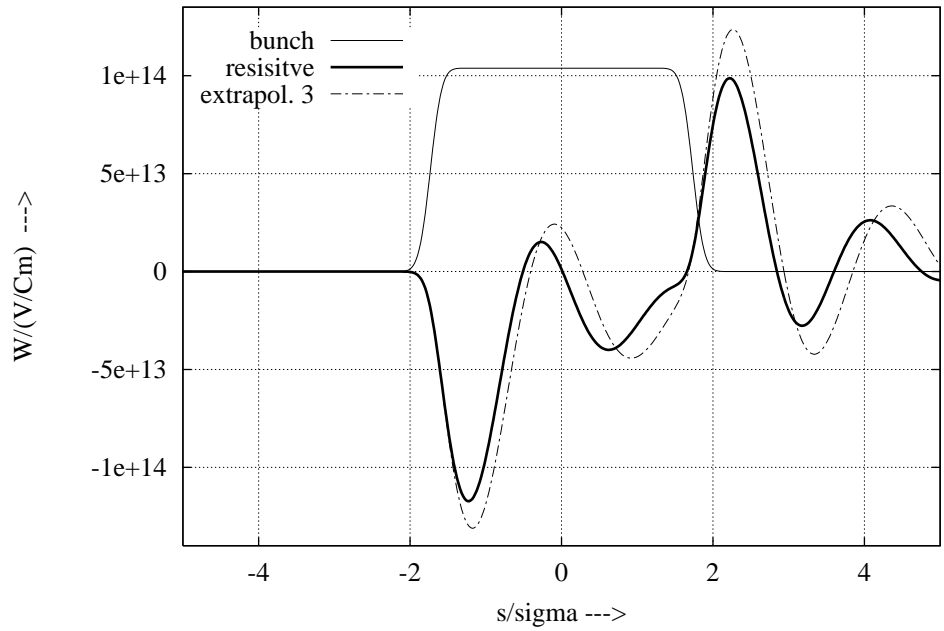


Fig. 31: Wake potential of a more rectangular bunch (solid line) calculated by the LB-N,2nd method (dot dashed line) , resistive wall wake (thick line) of a perfect pipe. Configuration: aluminum pipe, $R_0 = 5$ mm , random surface, bunch shape see text